REPORT

Bi-allelic *HPDL* Variants Cause a Neurodegenerative Disease Ranging from Neonatal Encephalopathy to Adolescent-Onset Spastic Paraplegia

Ralf A. Husain,[1,31] Mona Grimmel,[2,31] Matias Wagner,[3,4,5] J. Christopher Hennings,[6] Christian Marx,[7] René G. Feichtinger,[8] Abdelkrim Saadi,[9] Kevin Rostásy,[10] Florentine Radelfahr,[11,12] Andrea Bevot,[13] Marion Döbler-Neumann,[13] Hans Hartmann,[14] Laurence Colleaux,[15] Isabell Cordts,[16] Xenia Kobeleva,[17] Hossein Darvish,[18] Somayeh Bakhtiari,[19] Michael C. Kruer,[19] Arnaud Besse,[20] Andy Cheuk-Him Ng,[21] Diana Chiang,[21] Francois Bolduc,[21] Abbas Tafakhori,[22] Shrikant Mane,[23] Saghar Ghasemi Firouzabadi,[24] Antje K. Huebner,[6] Rebecca Buchert,[2] Stefanie Beck-Woedl,[2] Amelie J. Müller,[2] Lucia Laugwitz,[2,13] Thomas Nägele,[25] Zhao-Qi Wang,[7,26] Tim M. Strom,[3,4] Marc Sturm,[2] Thomas Meitinger,[3,4,27] Thomas Klockgether,[17,28] Olaf Riess,[2,29] Thomas Klopstock,[11,12,27] Ulrich Brandl,[1] Christian A. Hübner,[6] Marcus Deschauer,[16] Johannes A. Mayr,[8] Penelope E. Bonnen,[20] Ingeborg Krägeloh-Mann,[13,32] Saskia B. Wortmann,[3,4,8,30,32] and Tobias B. Haack[2,29,32,*]

We report bi-allelic pathogenic *HPDL* variants as a cause of a progressive, pediatric-onset spastic movement disorder with variable clinical presentation. The single-exon gene *HPDL* encodes a protein of unknown function with sequence similarity to 4-hydroxyphenylpyruvate dioxygenase. Exome sequencing studies in 13 families revealed bi-allelic *HPDL* variants in each of the 17 individuals affected with this clinically heterogeneous autosomal-recessive neurological disorder. HPDL levels were significantly reduced in fibroblast cell lines derived from more severely affected individuals, indicating the identified *HPDL* variants resulted in the loss of HPDL protein. Clinical presentation ranged from severe, neonatal-onset neurodevelopmental delay with neuroimaging findings resembling mitochondrial encephalopathy to milder manifestation of adolescent-onset, isolated hereditary spastic paraplegia. All affected individuals developed spasticity predominantly of the lower limbs over the course of the disease. We demonstrated through bioinformatic and cellular studies that HPDL has a mitochondrial localization signal and consequently localizes to mitochondria suggesting a putative role in mitochondrial metabolism. Taken together, these genetic, bioinformatic, and functional studies demonstrate HPDL is a mitochondrial protein, the loss of which causes a clinically variable form of pediatric-onset spastic movement disorder.

The group of pediatric neurological syndromes that include spasticity as the primary feature range from severe spastic movement disorders with onset in infancy to uncomplicated juvenile-onset hereditary spastic paraplegia (HSP). This group of disorders presents challenges to diagnostic paradigms due to large clinical variability and genetic heterogeneity. Delineation of the molecular bases underlying these diseases is necessary for informed decision making and counselling of affected individuals and their families. In addition, there is an increasing number of disorders especially among the inborn errors of metabolism, in which an adjusted clinical management or even new therapeutic approaches directly targeting the pathomechanism convincingly demonstrated

[1]Department of Neuropediatrics, Jena University Hospital, 07747 Jena, Germany; [2]Institute of Medical Genetics and Applied Genomics, University of Tuebingen, 72076 Tübingen, Germany; [3]Institute of Human Genetics, Technical University of Munich (TUM), School of Medicine, 81675 Munich, Germany; [4]Institute of Human Genetics, Helmholtz Zentrum München, 85764 Neuherberg, Germany; [5]Institute of Neurogenomics, Helmholtz Zentrum München, 85764 Neuherberg, Germany; [6]Institute of Human Genetics, Jena University Hospital, 07747 Jena, Germany; [7]Leibniz Institute on Aging - Fritz Lipmann Institute (FLI), 07745 Jena, Germany; [8]University Children's Hospital, Salzburger Landeskliniken (SALK) and Paracelsus Medical University (PMU), 5020 Salzburg, Austria; [9]Department of Neurology, Ben Aknoun Hospital, Benyoucef Benkhedda University, 16028 Algiers, Algeria; [10]Department of Pediatric Neurology, Children's Hospital Datteln, Witten/Herdecke University, 45711 Datteln, Germany; [11]Department of Neurology, Friedrich-Baur-Institute, Ludwig-Maximilians-University, 80336 Munich, Germany; [12]German Center for Neurodegenerative Diseases (DZNE), 81377 Munich, Germany; [13]Department of Pediatric Neurology and Developmental Medicine, University Children's Hospital, 72072 Tübingen, Germany; [14]Clinic for Pediatric Kidney-, Liver- and Metabolic Diseases, Hannover Medical School, 30625 Hannover, Germany; [15]INSERM UMR1163, Developmental Brain Disorders Laboratory, Imagine Institute, Paris-Descartes University, Paris, France; [16]Department of Neurology, Technische Universität München, School of Medicine, 81675 Munich, Germany; [17]Department of Neurology, University of Bonn, 53127 Bonn, Germany; [18]Cancer Research Center and Department of Medical Genetics, School of Medicine, Semnan University of Medical Sciences, Semnan, Iran; [19]Barrow Neurological Institute, Phoenix Children's Hospital & University of Arizona College of Medicine, Phoenix, AZ 85004, USA; [20]Department of Molecular and Human Genetics, Baylor College of Medicine, Houston, TX 77030, USA; [21]Division of Pediatric Neurology, Department of Pediatrics, University of Alberta, Edmonton, AB T6G 2R3, Canada; [22]Iranian Center of Neurological Research, Neuroscience Institute, Tehran University of Medical Sciences, Tehran, Iran; [23]Yale Center for Genome Analysis, Yale University School of Medicine, West Haven, CT 06516, USA; [24]Genetics Research Center, University of Social Welfare and Rehabilitation Sciences, Tehran, Iran; [25]Department of Neuroradiology, University Hospital Tuebingen, 72072 Tübingen, Germany; [26]Faculty of Biological Sciences, Friedrich Schiller University Jena, 07743 Jena, Germany; [27]Munich Cluster for Systems Neurology (SyNergy), 81377 Munich, Germany; [28]German Center for Neurodegenerative Diseases (DZNE), 53127 Bonn, Germany; [29]Centre for Rare Diseases, University of Tuebingen, 72076 Tübingen, Germany; [30]Radboud Center for Mitochondrial Medicine, Department of Pediatrics, Amalia Children's Hospital, Radboudumc, 6525 GA Nijmegen, the Netherlands
[31]These authors contributed equally to this work
[32]These authors contributed equally to this work
*Correspondence: tobias.haack@med.uni-tuebingen.de
https://doi.org/10.1016/j.ajhg.2020.06.015.

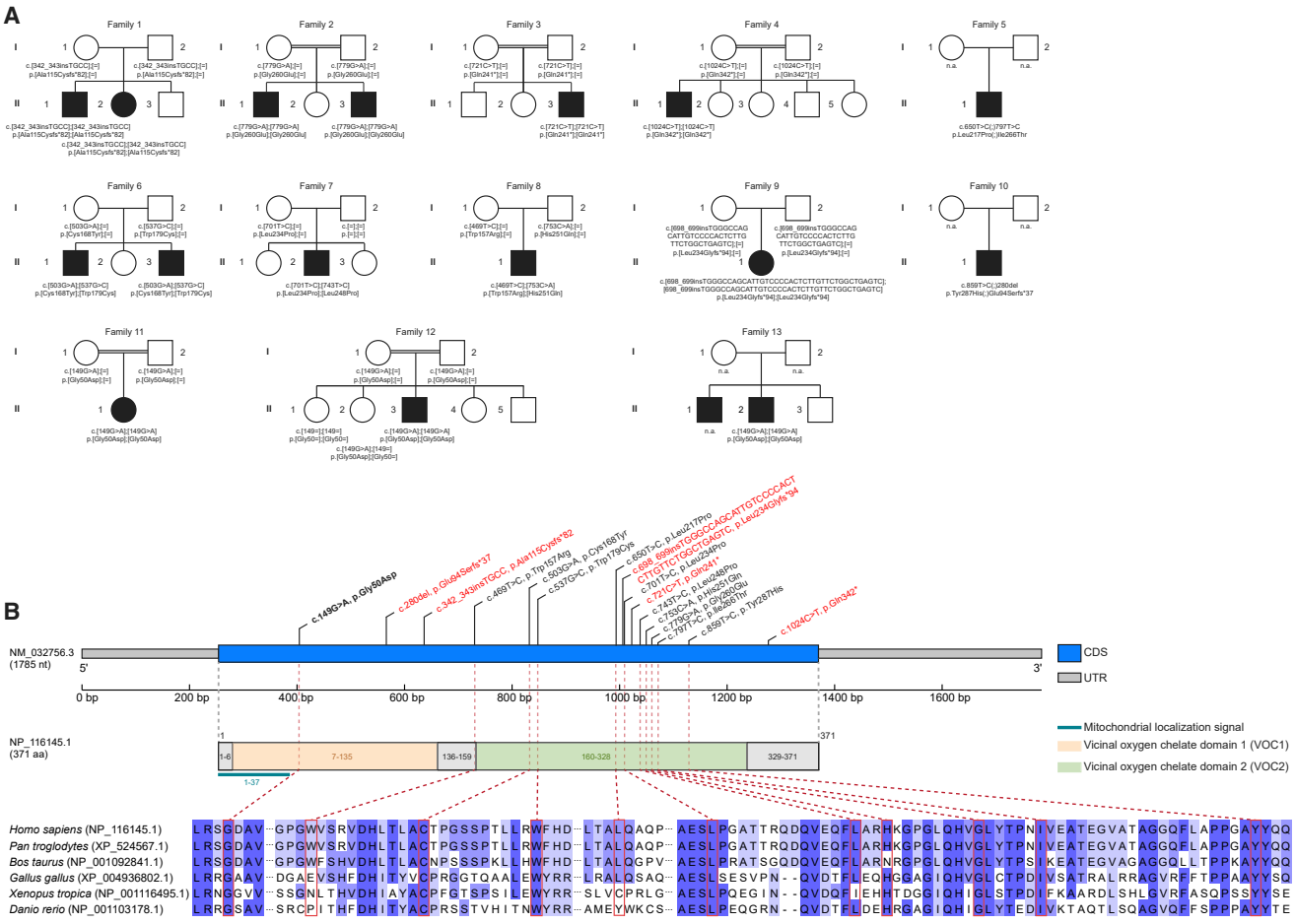

Figure 1. Pedigrees of Investigated Families and Structure of *HPDL*

(A) Pedigrees of 13 families with pathogenic variants in *HPDL*, illustrating the variant carrier status of affected (closed symbols) and healthy (open symbols) family members. Unaffected siblings were not tested unless indicated. n.a., not available for testing.

(B) Gene structure of *HPDL* and structure of the encoded protein with predicted domains of the gene product, mitochondrial localization signal, position of the identified variants, and conservation of affected amino acids across different species. The recurrent variant c.149G>A (p.Gly50Asp) is shown in bold; truncating variants are shown in red. Of note, evidence of the predicted N-terminal VOC domain is rather unclear as it partially overlaps with the mitochondrial localization signal which is expected to be cleaved off. CDS, coding sequence; UTR, untranslated region.

amelioration of clinical signs and symptoms.[1] Although exome and full genome sequencing significantly increased the diagnostic rate in clinical routine, estimates suggest that at least half of the severely affected pediatric cases remain undiagnosed.[2] One explanation among many others is a still incomplete list of disease-associated loci. We report on bi-allelic variants in *HPDL* that cause a spastic movement disorder with broad clinical variability and describe the full range of clinical manifestations resulting from pathogenic *HPDL* variants. *HPDL* is a single-exon gene that encodes a 371 amino acid protein (HPDL [GenBank: NP_116145.1]) of unknown function that is conserved across vertebrates (Figure 1).

Clinical characterization, molecular genetic, bioinformatic, and cell-based functional studies were conducted in 13 families with individuals clinically diagnosed with a pediatric-onset neurological syndrome ranging from a severe spastic movement disorder to uncomplicated HSP. The study was approved by the local ethics committees and informed consent was obtained from all affected individuals or their guardians.

Consanguinity was reported for parents of families F2, F3, F4, F11, and F12 (5 of 13 families, 38%). Pregnancy and postnatal adaption were reportedly normal in all 17 affected individuals. All individuals in this study are alive with current ages ranging from 1 7/12 years to 39 years. Frequently observed clinical findings included chronic progression of neurological signs (n = 16/17, 94%), motor developmental delay (n = 12/17, 71%), intellectual impairment (n = 11/17, 65%), microcephaly (n = 9/16, 56%), and seizures/epilepsy (n = 9/17, 53%). Other relevant clinical findings were visual disturbances/strabismus (n = 9/17, 53%) and loss of developmental milestones (n = 6/17, 35%). Acute central respiratory failure leading to life-threatening events requiring partly mechanically assisted ventilation occurred in half of individuals with infantile presentation (n = 5/10, 50%), respectively one third of all individuals (n = 5/17, 29%). These apnoeas with hypercapnia appeared

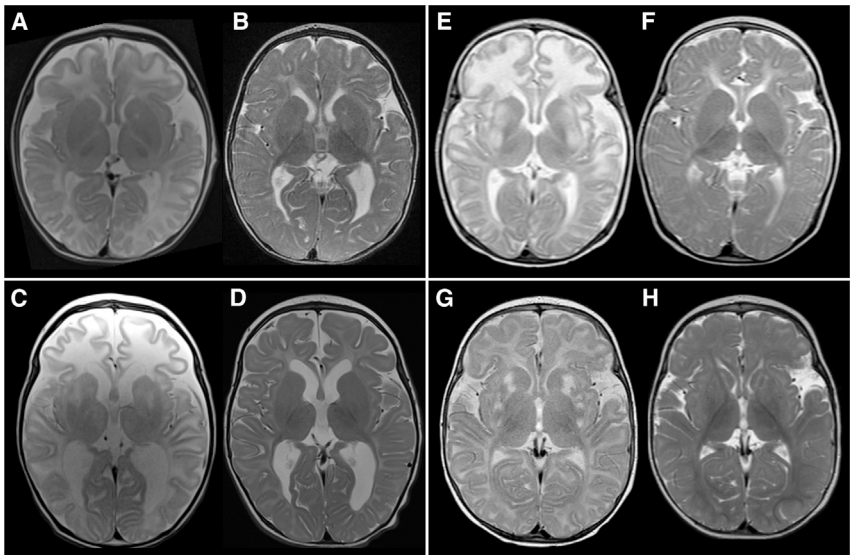

Figure 2. MRI Pattern I
MRIs (T_2-weighted axial scans) from individual F6:II.1 at 2 and 15 months of age (A, B), individual F6:II.3 at 1 1/2 and 7 months of age (C, D), individual F7:II.2 at 2 and 12 months of age (E, F), and individual F8:II.1 at 5 and 12 1/2 months of age (G, H). Early imaging shows multifocal signal increase in the striatum in all individuals, in part associated with swelling (E). With the exception of individual F8:II.1 (G, H), white matter shows abnormal high signal especially in the frontal lobes. On follow-up, myelination in these three individuals is delayed and white matter volume reduced (best seen in B and D).
Summary: after early infantile pathology in the striatum and in part also white matter, follow-up indicates remission of striatal changes, variable progress of myelination, and white matter atrophy if white matter was initially abnormal.

in early infancy (3 resp. 6 weeks of age; F6:II.1 and F6:II.3), childhood (age not specified, F2:II.3), as well as school age (7 and 11 years of age; F4:II.1 and F3:II.3, respectively) with a duration of several days to weeks and without recurrence except in individual F2:II.3 who had two episodes. In individual F3:II.3, acute respiratory failure was reportedly associated with an infection. Demyelinating neuropathy was present in three individuals (n = 3/11, 27%), with reduced sensory nerve conduction velocity (NCV) in all and severely reduced motor NCV in one. Dysmorphic features were documented with high-arched palate and hypertelorism in the two brothers from family F1, a long philtrum and low-set ears in individual F7:II.2, and 2-3 toe syndactyly in individual F11:II.1 (n = 4/17, 24%).

In summary, we observed a spectrum of neurologic impairment ranging from a severe congenital form without any neurological development (n = 2/17, 12%) to infantile-onset presentations (n = 10/17, 59%) with moderate to severe neurodevelopmental issues, partly with a pathology reminiscent of mitochondrial disease (Leigh-like syndrome), to juvenile-onset spastic paraplegia (n = 5/17, 29%).

Elevated lactate in blood (range 2.7–7.9 mmol/l) and/or CSF (range 2.3–8.2 mmol/l) was present in 9 out of 11 (82%) individuals with respective measurements mostly at times of neurologic deterioration but not during check-ups in stable condition. Extensive laboratory testing and metabolic investigations were non-contributory in individuals with corresponding measurements (n = 8/15, 53%). In particular, metabolites of tyrosine degradation (i.e., tyrosine, 4-hydroxyphenylpyruvate) upstream to the HPDL paralog enzyme HPD were normal in blood (n = 7), urine (n = 6), and CSF (n = 6). Moreover, liquid chromatography quadrupole time-of-flight mass spectrometry (LC-QToF-MS) in CSF did not show elevation of tyrosine pathway metabolites (n = 3).[3]

Histology of skeletal muscle displayed fiber size variation in 3 out of 5 (60%) examined individuals. Activities of mitochondrial respiratory chain complexes were variably reduced in skeletal muscle in 2 out of 5 (40%) individuals (Table S1) but not reduced in fibroblasts cell lines from 4 affected individuals (Table S2).

MRI studies of the brain and spinal cord were available for review from 12 and 5 individuals, respectively, in part with longitudinal studies; MR spectroscopy (MRS) was performed on 4 individuals with infantile onset showing elevated lactate peaks in 3 of them (75%). We suggest that three major neuroradiological patterns associated with HPDL deficiency can be delineated (see Figures 2, 3, S1, and S2).

MRI Pattern I (individuals F6:II.1, F6:II.3, F7:II.2, F8:II.1) was characterized by bilateral multifocal striatal signal changes (best seen on T_2-weighted scans), in part with some swelling as well as increased lactate level in MRS in one individual (F6:II.3) evoking a certain acuity. In all but one individual (F8:II.1), myelination was deficient and white matter signal clearly abnormal, indicating white matter pathology. On follow-up, the basal ganglia changes disappeared or were regressive, and an atrophy of the white matter was observed in two individuals (F6:II.1, F6:II.3), although there was some progress in myelination. Two individuals (F7:II.2, F8:II.1) had no atrophy and good myelination progress on follow-up.

Two individuals (F1:II.1 and F1:II.2) with MRI Pattern I Suspected showed severe white matter and corpus callosum volume reduction with parieto-occipital predominance at age 5 (F1:II.1) and 7 (F1:II.2) years (Figure S1). Myelination was deficient; U-fibers particularly were not myelinated (T_2-weighted scans). Cerebellum appeared normal. Taken into account the very early onset of the disease characterized by primary developmental delay and severe neurological signs, and the similarity of MRIs with the later MRI pathology of the two more severely affected individuals with MRI Pattern I (F6:II.1 and F6:II.3), we chose to call this pattern with severe white matter atrophy and deficient myelination MRI Pattern I Suspected,

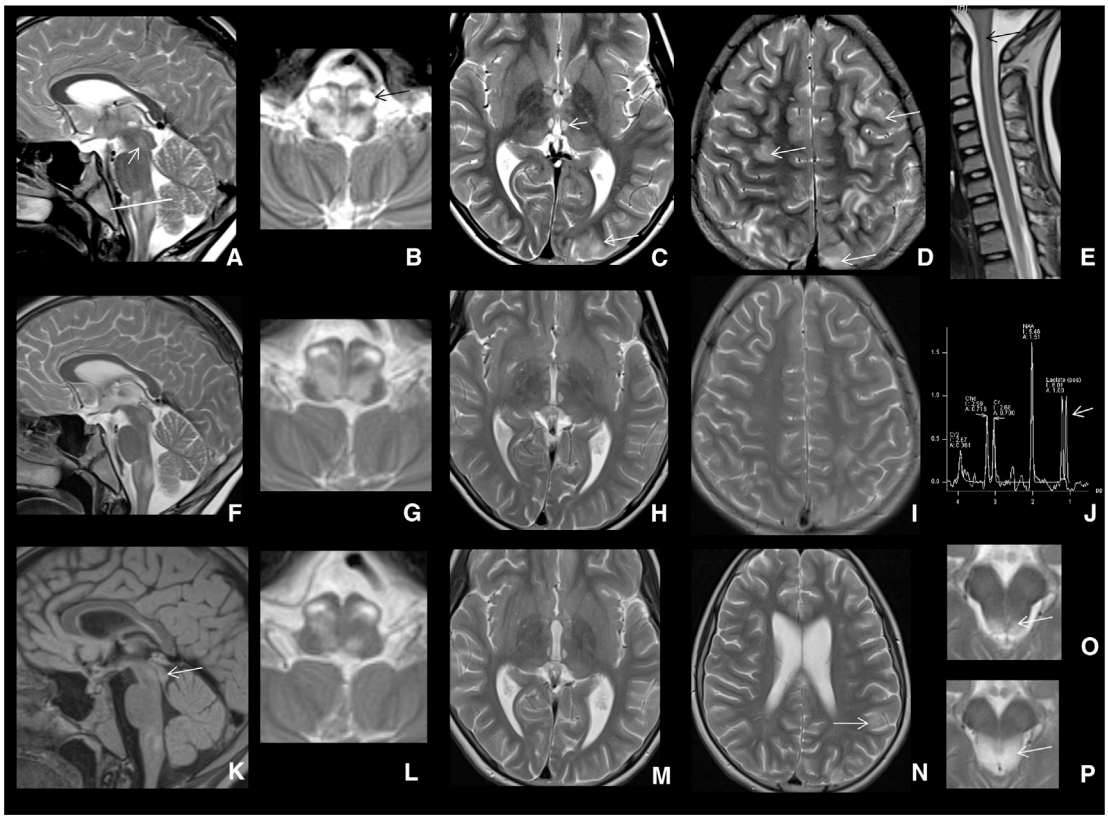

Figure 3. MRI Pattern II

MRIs (T_2-weighted sagittal and axial scans) from individual F3:II.3. At the age of 10 11/12 years (A–E), extensive brain stem involvement is apparent, especially of the olivae (black arrow in B, white line in sagittal image in A indicates position of brainstem in axial image B). The sagittal image also shows diffuse signal changes of the diencephalon and periaquaeductal gray (arrow in A). In the thalamus, distinct changes of the mediodorsal thalamic nuclei are evident (C, short white arrow). Multifocal cortico-subcortical signal changes are indicated by white arrows (C, D). Sagittal images of the spinal cord indicate mild signal increase centrally, most pronounced cervically (black arrow in E). Six days later (F–J), signal changes are overall less prominent and MRS in the frontoparietal white matter shows a lactate peak (arrow, J). At the age of 11 years (K–N), signal changes are further receding, still apparent in colliculi inferiores (arrow in K), brain stem (L), mediodorsal thalamus (M), and some cortical areas (mostly parietal left, arrow in N). Two images of the inferior colliculi at the age of 11 5/12 years (O) and 11 10/12 years (P) show a new pathology bilaterally, getting more prominent and swollen.

Summary: at 11 years of age widespread and acute changes of cortex, thalamus, brain stem, and spinal cord, receding with residual changes in the brain stem; over the course of 11 months, a new pathology appears in the inferior colliculi.

arguing that the early MR signs of MRI Pattern I might have been missed.

MRI Pattern II was observed in two individuals (F3:II.3 and F4:II.1) who showed predominantly brain stem and medioposterior thalamic changes, remitting and relapsing with acute changes of the inferior colliculi. One individual (F4:II.1) also showed cerebellar white matter changes (T_2-weighted scans) as well as increased lactate in the frontoparietal white matter in MRS and the other (F3:II.3) presented with cortico-subcortical changes, which showed in part remission, but relapsed with additional brain stem and inferior colliculi changes. It seems remarkable that no relevant diffusion changes were observed in any affected individual, even when other acute changes were detected.

MRI Pattern III is not related to clear pathology and was found in three individuals (F9:II.3, F11:II.1, and F12:II.3). In one individual (F9:II.3), there was suspicion of long extended central signal changes (T_2-weighted scans) of the spinal cord, which, however, was not confirmed in a follow-up MRI 2 weeks later. Thus, a quickly regressive mild spinal pathology cannot be excluded.

Clinical and genetic findings are summarized in Table 1, pedigrees are shown in Figure 1, and neuroimaging findings are in Figures 2, 3, S1, and S2. Detailed clinical descriptions are provided in the Supplemental Note.

Exome sequencing and analysis were performed at five centers (Tuebingen for families F4, F6, F8, F9, F12, and F13; Munich for families F3, F7, and F11; Baylor for families F5 and F10; Paris for family F1; and Phoenix for family F2) on genomic DNA from individuals F1:II.1, F1:II.2, F2:II.1, F2:II.3, F3:II.3, F4:II.1, F5:II.2, F6:II.1, F6:II.3, F7:II.2, F8:II.1, F9:II.1, F10:II.1, F11:II.1, F12:II.3, and F13:II.2, as well as parental samples from families F3, F4, F6, F8, and F12 as described previously.[4–10] The cohort was assembled using GeneMatcher[11] for families F1, F2, F3, F7, and F11 and by discussion between collaborators for families F4, F5, F6, F8, F9, F10, F12, and F13.

Table 1. Clinical and Genetic Findings in Individuals with Bi-allelic *HPDL* Variants

Individual	F1: II.1	F1:II.2	F2: II.1	F2: II.3	F3: II.3	F4: II.1	F5: II.2	F6: II.1	F6: II.3	F7: II.2	F8: II.1	F9: II.1	F10: II.1	F11: II.1	F12: II.3	F13: II.1	F13: II.2
Gender	M	F	M	M	M	M	M	M	M	M	M	F	M	F	M	M	M
Country of origin	Algeria	Algeria	Iran	Iran	Turkey	Syria	Canada	Ger many	Ger many	Ger many	Ger many	Ger many	USA	Turkey	Syria	Turkey	Turkey
cDNA change[a] variant 1	c.342_343 insTGCC	c.342_343 insTGCC	c.779 G>A	c.779 G>A	c.721 C>T	c.1024 C>T	c.650 T>C	c.503 G>A	c.503 G>A	c.701 T>C	c.469 T>C	c.698_699 insTGGGCC AGCATTG TCCCCACT CTTGTTCT GGCTGAGTC	c.280 del	c.149 G>A	c.149 G>A	N/D	c.149 G>A
Protein change[b] variant 1	p.Ala115 Cysfs*82	p.Ala115 Cysfs*82	p.Gly 260Glu	p.Gly 260Glu	p.Gln 241*	p.Gln 342*	p.Leu 217Pro	p.Cys 168Tyr	p.Cys 168Tyr	p.Leu 234Pro	p.Trp 157Arg	p.Leu234 Glyfs*94	p.Glu94 Serfs*37	p.Gly 50Asp	p.Gly 50Asp	N/D	p.Gly 50Asp
cDNA change[a] variant 2	homo zygous	homo zygous	homo zygous	homo zygous	homo zygous	homo zygous	c.797 T>C	c.537 G>C	c.537 G>C	c.743 T>C	c.753 C>A	homo zygous	c.859 T>C	homo zygous	homo zygous	N/D	homo zygous
Protein change[b] variant 2	homo zygous	homo zygous	homo zygous	homo zygous	homo zygous	homo zygous	p.Ile 266Thr	p.Trp 179Cys	p.Trp 179Cys	p.Leu 248Pro	p.His 251Gln	homo zygous	p.Tyr 287His	homo zygous	homo zygous	N/D	homo zygous
Phenotype	congenital	congenital	infantile	infantile	infantile	infantile	infantile	infantile	infantile	infantile	infantile	infantile	juvenile	juvenile	juvenile	juvenile	juvenile
Age of onset/ current age	congenital/ 8 y	congenital/ 7 y	6 m/ 34 y	2 m/ 21 y	6 m/ 11 y	1 y/ 10 y	1 w/ 22 y	3 w/ 5 y	6 w/ 1 y 7 m	6 w/ 5 y	5 m/ 2 y	5 y/ 8.5 y	15 y/ 17 y	15 y/ 20 y	15 y/ 19 y	14 y/ 39 y	15 y/ 33 y
Delay of motor development	+	+	+	+	+	+	+	+	+	+	+	+	−	−	−	−	−
Intellectual impairment	+ (severe)	+ (severe)	+ (severe)	+ (severe)	+ (moderate)	+ (mild)	+	+ (mild)	N/A	+ (severe)	+ (mild)	+ (mild)	−	−	−	−	−
Chronic progression	+	+	+	+	+	+	+	+	+	−	+	+	+	+	+	+	+
Regression	−	−	+	+	+	+	+	−	−	−	−	+	−	−	−	−	−
Acute respiratory failure (age)	−	−	−	+ (2 x childhood)	+ (11 y)	+ (7 y)	−	+ (3 w)	+ (6 w)	−	−	−	−	−	−	−	−
Microcephaly (SD)	+ (−5.3)	+ (−5.0)	+ (−4.6)	+ (−5.3)	−	−	−	+ (−3.3)	+ (−4.2)	+ (−2.5)	+ (−2.2)	+ (−2)	−	N/D	−	−	−
Seizures	+	+	+	+	+	−	+	+	+	+	−	−	−	−	−	−	−
Spastic paraplegia	+ (tetraparesis)	+ (tetraparesis)	+ (tetraparesis)	+ (tetraparesis)	+	+	+	+	+	+	+	+	+	+	+	+	+

(*Continued on next page*)

Table 1. ***Continued***

Individual	F1: II.1	F1:II.2	F2: II.1	F2: II.3	F3: II.3	F4: II.1	F5: II.2	F6: II.1	F6: II.3	F7: II.2	F8: II.1	F9: II.1	F10: II.1	F11: II.1	F12: II.3	F13: II.1	F13: II.2
Visual disturbance	+	+	−	−	+	+	+	+	+	−	+	−	−	−	−	+	−
MRI pattern	pattern I suspected	pattern I suspected	N/D	pattern I suspected	pattern II	pattern II	#	pattern I	pattern I	pattern I	pattern I	pattern III	#	pattern III	pattern III	N/D	#
lactate increase (MRS)	N/D	N/D	N/D	N/D	+	+	N/D	N/D	+	N/D	−	N/D	N/D	N/D	N/D	N/D	N/D
Peak lactate blood; csf (mmol/l)	2.7; n	n; 6.2	N/D	N/D	5.2; 2.7	n; n	4.3; N/D	4.0; 6.9	7.9; 8.2	N/D; 3.8	4.3; 3.3	n; 2.3	N/D	n; N/D	n; n	N/D	N/D
Nerve conduction studies	n	n	n	n	n	severely reduced motor NCV, slightly reduced sensory NCV	N/D	reduced sensory NCV unilateral	reduced sensory NCV	N/D	N/D	N/D	N/D	n	n	n	N/D
Muscle histology	N/D	N/D	N/D	N/D	n	abnormal variation in muscle fiber diameter	N/D	N/D	n	abnormal variation in muscle fiber diameter	abnormal variation in muscle fiber diameter	N/D	N/D	N/D	N/D	N/D	N/D
Respiratory chain activities (muscle)	N/D	N/D	N/D	N/D	n	globally reduced (CI-CV)	N/D	N/D	CIV-deficiency	n	n	N/D	N/D	N/D	N/D	N/D	N/D
Respiratory chain activities (fibroblasts)	n (CIII/CV increased)	N/D	N/D	N/D	N/D	n (CIII/CV increased)	N/D	N/D	n (CV increased)	N/D	n	N/D	N/D	N/D	N/D	N/D	N/D

M, male; F, female; y, years; m, months; w, weeks; n, normal; N/A, not applicable; N/D, not done/determined; MRS, MR spectroscopy; NCV, nerve conduction velocity; +, present; −, absent; #, MRI not available for review.
[a]GenBank: NM_032756.3
[b]GenBank: NP_116145.1

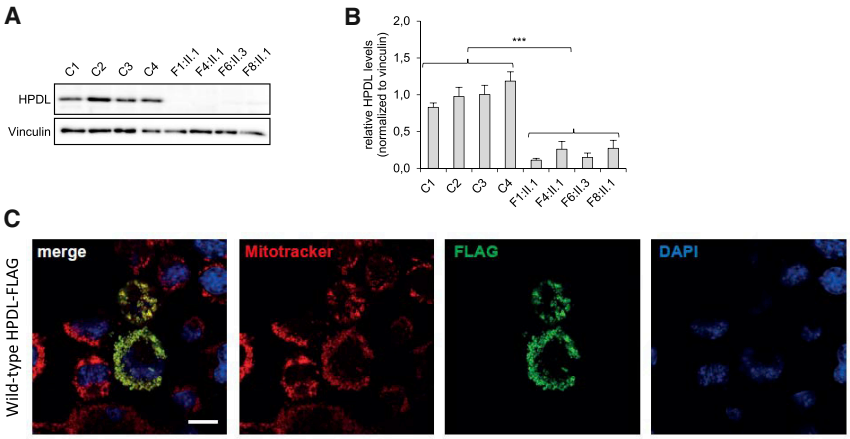

Figure 4. HPDL Protein Levels and Subcellular Localization

(A) Investigation of HPDL protein levels by immunoblot analysis with a polyclonal antibody against full-length HPDL (for detailed methods see Figure S5). HPDL was detected in fibroblasts of control subjects but was significantly reduced in fibroblasts of affected individuals F1:II.1, F4:II.1, F6:II.3, and F8:II.1.

(B) Protein levels were quantified from HPDL immunoblots shown in Figure S5 using ImageJ (NIH). The graph displays the average of three individual experiments ± SEM. Statistics were done using two-tailed t test of the average of the control group compared to the average of affected individuals. ***$p < 0.001$.

(C) Overexpression of *HPDL* cDNA with a C-terminal FLAG tag in N2a cells. Wild-type *HPDL* cDNA was transiently overexpressed and detected by FLAG immunostaining. Mitochondria were stained with Mitotracker and nuclei were stained with DAPI. HPDL co-localizes with the mitochondria. Scale bar = 10 μm.

Clinical genetic diagnostic testing did not reveal pathogenic or likely pathogenic variants in genes that have been associated with the affected individuals' clinical phenotypes and deeper analysis of exome data was subsequently conducted. Due to the presence of consanguinity in several families, rare, bi-allelic non-synonymous variants were prioritized. Variant filtering criteria included minor allele frequency threshold < 0.001, without homozygous occurrence in the Genome Aggregation Database (gnomAD v.2.1.1) as well as in-house exome and genome datasets from individuals with unrelated phenotypes. This search led us to prioritize bi-allelic variants in *HPDL* in all affected individuals ($n = 17$) in this cohort of 13 unrelated families (Figure 1). No homozygous loss-of-function variants in *HPDL* were listed in gnomAD (v.2.1.1) or individuals with unrelated phenotypes in in-house databases. Segregation analyses on available family members showed full co-segregation of the identified bi-allelic *HPDL* variants with the clinical status in all families (Figure 1A).

The 17 affected individuals were either homozygous or compound heterozygous for ultra-rare variants in *HPDL* (Table 1). Across these 17 affected individuals, 16 *HPDL* unique variants were identified, only one of which was observed in gnomAD: the missense variant *HPDL* (GenBank: NM_032756.3): c.149G>A (p.Gly50Asp) was detected twice in a heterozygous state in the non-Finnish European population and has an allele frequency of 1e−5 in the total gnomAD population. Five of the identified variants are nonsense variants. Given that *HPDL* is a single-exon gene, the mutant messenger RNAs are likely to escape nonsense-mediated decay resulting in a prematurely truncated polypeptide and loss of HPDL function. A total of 11 *HPDL* missense variants were observed in this cohort. All missense variants affect evolutionarily conserved amino acids, with most of them being highly conserved (phyloP), and are predicted pathogenic *in silico* (10/11 variants predicted deleterious with SIFT score ≤ 0.01, 9/11 variants predicted probably damaging with PolyPhen score > 0.9, CADD score > 18 for 11/11 variants and > 25 for 8/11 variants) (Figure 1, Table S3).

One missense variant, c.149G>A (p.Gly50Asp), was observed in a homozygous state in four affected individuals from the three families F11, F12, and F13. Concordant with the reported consanguineous relationships in families F11 and F12 and a presumed distant relatedness in family F13, we detected extended runs of homozygosity (ROH) including ~8.4 Mb, ~4.9 Mb, and ~3.3 Mb of ROH encompassing *HPDL*. These families originate from neighboring geographic regions in Turkey and Syria. The analysis of the genomic region surrounding *HPDL* showed that the affected individuals from these families share the same homozygous common variants over a 1.9 Mb region that traverses *HPDL* and includes 58 segregating variants with the respective positions being covered in all three exome datasets (Table S4). These data are in line with a distant shared ancestry among these families.

Of note, the missense variant c.149G>A (p.Gly50Asp) is consistently associated with isolated spastic paraplegia evolving in the second decade of life and currently no additional pathologies. Apart from one additional individual with a juvenile presentation (F10:II.1), the remaining affected individuals reported in this study had a more severe, infantile-onset disease presentation. We speculate that the milder clinical presentation observed in a subset of affected individuals with predominant spastic paraplegia evolving in the second decade of life might result from putative residual activities in some HPDL mutants. However, at the time of the study no biomaterials from any of these individuals were available to confirm the postulated presence of residual amounts of HPDL. Furthermore, to our knowledge, the molecular function of HPDL is currently unknown and the lack of a direct test for HPDL function or biomarker currently prevents a detailed evaluation of correlations between genotypes, residual protein function, and phenotypic spectrum.

We tested the hypothesis that *HPDL* variants detected in severely affected individuals caused loss of function.

Fibroblast cell lines were available from four affected individuals, F1:II.1, F4:II.1, F6:II.3, and F8:II.1, to perform additional studies to test the functional relevance of identified variants. Western blot analyses showed a significant reduction in HPDL protein levels in fibroblasts from affected individuals compared to control fibroblasts (Figure 4). This result demonstrates that the *HPDL* variants detected in these individuals resulted in the severe reduction of HPDL protein. Given that the mutant mRNA of the single-exon gene *HPDL* should escape nonsense-mediated decay, the nonsense variants detected in individuals F1:II.1 and F4:II.1 presumably lead to a loss of HPDL via impaired protein stability. The other two individuals tested here, F6:II.3 and F8:II.1, were compound heterozygous for missense variants and our results indicate that, similar to nonsense variants, the identified missense changes result in loss of function of HPDL (Figure S5). We hypothesize that these missense changes result in loss of HPDL through impaired production or stability of the HPDL protein.

HPDL is present in various tissues with particularly high levels in the central and peripheral nervous system (GTEx Analysis Release V.8, dbGaP Accession phs000424.v8.p2 on 03/10/2020). The function of HPDL is currently unknown. Bioinformatic analysis shows that HPDL belongs to the vicinal oxygen chelate (VOC) superfamily. VOC members are metalloenzymes with diverging sequence and biological functions, commonly sharing a βαββββ structural motif (VOC fold), that form an incompletely closed barrel of β sheet around a metal ion.[12] The Human Protein Atlas reports HPDL as having mitochondrial localization, based on antibody-based profiling by immunofluorescence confocal microscopy.[13] However, HPDL is not present in the MitoCarta2.0, which is a database of 1,158 human proteins with mass-spectometry-based evidence of localization to the mitochondria.[14] To resolve these conflicting reports, we carried out bioinformatic and functional studies. First, we conducted bioinformatic analysis, using MitoProt II, to determine if the HPDL protein sequence contains a mitochondrial localization signal.[15] MitoProt II predicts that the first 37 amino acids of HPDL comprise a mitochondrial localization signal (Figure 1), with 98% probability. Next, we overexpressed wild-type *HPDL* cDNA in a murine Neuro 2A cell line and performed immunohistological studies visualizing HPDL with a C-terminal FLAG tag. The results of these experiments demonstrate that HPDL co-localizes with the mitochondria as shown in Figure 4.

Having established a mitochondrial localization of HPDL, we assessed whether HPDL might play a role in oxidative phosphorylation (OXPHOS) and whether loss of HPDL leads to disruption of the mitochondrial network. Investigation of mitochondrial morphology in fibroblasts from affected individuals visualized by Mitotracker Red CMXRos staining and data analysis with the Mitochondrial Network Analysis (MiNA[16]) tool showed no significant differences between control and fibroblast cell lines from affected individuals (n = 2/2, Figures S3 and S4). As stated previously, analyses of the OXPHOS component enzyme activities showed mostly normal activities in fibroblasts from affected individuals (n = 4, Table S2). In line with this observation, immunofluorescence studies in fibroblasts from affected individuals of OXPHOS subunits including NDUFS4, SDHA, UQCRC2, MT-CO1, and ATP5F1A (data not shown) as well as immunoblot analysis of NDUFB8, SDHB, UQCRC2, COX IV, and ATP5A in fibroblasts from affected individuals (Figure S6) failed to show any consistent abnormalities. Analysis of OXPHOS complexes in available skeletal muscle specimen revealed variably decreased activities of complexes I and/or IV in some individuals (n = 2/5, Table S2). Muscle biopsies were reported displaying abnormal variation in muscle fiber diameter in the majority of investigated cases (n = 3/5, 60%, data not shown). Immunohistochemical staining of muscle tissue from two affected individuals (F4:II.1 and F6:II.3) indicated overall lower levels of mitochondrial/OXPHOS proteins (VDAC1, SDHA, and MT-CO1) in comparison to control subjects (Figure S7), whereby it was remarkable that large muscle bundles of F4:II.1 had a depletion of mitochondria. Consistent with this observation, western blot analyses of muscle tissue showed a general lack of OXPHOS enzymes in F4:II.1 but not in F8:II.1 (Figure S8). Together, these data fail to establish a consistent signature of OXPHOS impairment or mitochondrial dysmorphology in the investigated fibroblasts or muscle from affected individuals.

In summary, the identification of 16 different bi-allelic functionally relevant *HPDL* variants in 17 affected individuals from 13 unrelated families establishes *HPDL* as a gene confidently implicated in this neurological disorder. In all individuals a spastic movement disorder predominantly of the lower limbs was observed as a common clinical sign. However, disease onset and progress as well as the spectrum of accompanying phenotypes were highly variable. The most severely affected individuals had a congenital disease onset with primary microcephaly and severe developmental delay but without clearly progressive neurological signs and an overall stable disease course. Affected individuals with infantile-onset disease manifested first signs and symptoms after weeks, months or even years of apparently normal development. Clinical and neuroimaging findings in these individuals initially resembled mitochondrial encephalopathies. However, compared with other forms of mitochondrial disease, such as complex I-associated Leigh syndrome, the further clinical course seems to be more stable resulting in a spastic movement disorder with additional features such as intellectual disability, epilepsy, swallowing problems, and peripheral neuropathy. A third group includes individuals who are homozygotes for the missense change c.149G>A (p.Gly50Asp) that develop hereditary spastic paraplegia between the ages of 14 and 15 years without obvious abnormalities in brain and spinal MRI or additional clinical features. Our study highlights the broad heterogeneity of clinical features associated with HPDL deficiency rendering this disorder an important differential diagnosis for a substantial fraction of clinical conditions managed by pediatric as well as adult neurologists. However, further

studies and long-term follow-up of affected HPDL individuals are needed to fully define the phenotypic spectrum and natural disease course associated with HPDL deficiency. Of note, the disease course of several individuals is compatible with a relatively acute exacerbation of the disease followed by a static encephalopathy and development of a residual clinical status hallmarked by a spastic movement disorder. Comparable disease courses are known from other metabolic disorders including ECHS1 deficiency, a defect presumably exerting its effect due to accumulation of toxic metabolites and secondary impairment of the OXPHOS machinery and mitochondrial metabolism.[17] Along this line, acute episodes might be triggered by external factors such as infection or nutritional status and vice versa might be amenable to early symptomatic or even dietary intervention. Key to the development of any therapeutic approach is a better understanding of the physiological function of HPDL and, if deficient, the downstream molecular cascades causing pathology. Our clinical observations and functional studies suggest an involvement of mitochondrial metabolism in the pathogenesis of the disease. These include biochemical features like elevated lactate and alanine in body fluids, neuroimaging findings with bilateral signal alterations of the basal ganglia and brain stem, lactate elevation in MR spectroscopy, as well as experimental evidence of a mitochondrial localization of HPDL. However, we did not observe a consistent signature of mitochondrial dysfunction in HPDL mutant fibroblasts and skeletal muscle. As stated above, a potential explanation could be that mitochondrial function is only secondarily impaired during acute episodes of the disease and cannot be directly confirmed at later time points *in vivo* or by using *in vitro* model systems such as fibroblast cell lines. Furthermore, the clinically predominantly affected organ is the brain and probably more advanced approaches such as neuronal cell lines or organoids are needed to model and eventually understand HPDL deficiency in more detail.

Data and Code Availability

This study did not generate new code. Sequence datasets have been generated and contributed by different study sites and have not been deposited in a public repository due to varying local consent regulations. Selected datasets might be available from the corresponding author on request.

Supplemental Data

Supplemental Data can be found online at https://doi.org/10.1016/j.ajhg.2020.06.015.

Acknowledgments

We thank all families for their participation. We thank Karlien Coene, PhD, Department of Laboratory Medicine, Translational Metabolic Laboratory, Radboud University Medical Center, Nijmegen, the Netherlands for next-generation metabolic screening of CSF. T.B.H. was supported by the German Bundesministerium für Bildung und Forschung (BMBF) through the Juniorverbund in der Systemmedizin "mitOmics" (FKZ 01ZX1405C), the intramural fortüne program (#2435-0-0), and by the Deutsche Forschungsgemeinschaft (DFG, German Research Foundation) – Projektnummer (418081722). S.B.W. was supported by the Jubiläumsfonds of the OeNB Nr. 18023. J.A.M. was supported by the E-Rare project GENOMIT FWF-I2741B26. C.A.H. was supported by the BMBF (TreatHSP, FKZ 01GM1905D). F.R., T.M., and T. Klopstock were supported by a German Federal Ministry of Education and Research grant to the German Network for Mitochondrial Disorders (mitoNET, 01GM1113A, and 01GM1906A). P.E.B. was supported by NIH NINDS RO1 NS08372. Several authors of this publication are members of the European Reference Network for Rare Neurological Diseases - Project ID No 739510.

Declaration of Interests

The authors declare no competing interests.

Received: May 18, 2020
Accepted: June 22, 2020
Published: July 23, 2020

Web Resources

Ensembl Variant Effect Predictor, https://grch37.ensembl.org/Homo_sapiens/Tools/VEP
CADD, https://cadd.gs.washington.edu/
GenBank, https://www.ncbi.nlm.nih.gov/genbank/
gnomAD Browser, https://gnomad.broadinstitute.org/
GTEx Portal, https://gtexportal.org
MitoProt II, https://ihg.gsf.de/ihg/mitoprot.html
OMIM, https://www.omim.org/
The Human Protein Atlas, http://www.proteinatlas.org/
UCSC (February 2009), https://genome.ucsc.edu

References

1. Koch, J., Mayr, J.A., Alhaddad, B., Rauscher, C., Bierau, J., Kovacs-Nagy, R., Coene, K.L., Bader, I., Holzhacker, M., Prokisch, H., et al. (2017). CAD mutations and uridine-responsive epileptic encephalopathy. Brain *140*, 279–286.
2. Lionel, A.C., Costain, G., Monfared, N., Walker, S., Reuter, M.S., Hosseini, S.M., Thiruvahindrapuram, B., Merico, D., Jobling, R., Nalpathamkalam, T., et al. (2018). Improved diagnostic yield compared with targeted gene sequencing panels suggests a role for whole-genome sequencing as a first-tier genetic test. Genet. Med. *20*, 435–443.
3. Coene, K.L.M., Kluijtmans, L.A.J., van der Heeft, E., Engelke, U.F.H., de Boer, S., Hoegen, B., Kwast, H.J.T., van de Vorst, M., Huigen, M.C.D.G., Keularts, I.M.L.W., et al. (2018). Next-generation metabolic screening: targeted and untargeted metabolomics for the diagnosis of inborn errors of metabolism in individual patients. J. Inherit. Metab. Dis. *41*, 337–353.
4. Haack, T.B., Hogarth, P., Kruer, M.C., Gregory, A., Wieland, T., Schwarzmayr, T., Graf, E., Sanford, L., Meyer, E., Kara, E., et al. (2012). Exome sequencing reveals de novo WDR45 mutations causing a phenotypically distinct, X-linked dominant form of NBIA. Am. J. Hum. Genet. *91*, 1144–1149.

5. Ploski, R., Pollak, A., Müller, S., Franaszczyk, M., Michalak, E., Kosinska, J., Stawinski, P., Spiewak, M., Seggewiss, H., and Bilinska, Z.T. (2014). Does p.Q247X in TRIM63 cause human hypertrophic cardiomyopathy? Circ. Res. *114*, e2–e5.
6. Yang, Y., Muzny, D.M., Xia, F., Niu, Z., Person, R., Ding, Y., Ward, P., Braxton, A., Wang, M., Buhay, C., et al. (2014). Molecular findings among patients referred for clinical whole-exome sequencing. JAMA *312*, 1870–1879.
7. Fritzen, D., Kuechler, A., Grimmel, M., Becker, J., Peters, S., Sturm, M., Hundertmark, H., Schmidt, A., Kreiß, M., Strom, T.M., et al. (2018). De novo FBXO11 mutations are associated with intellectual disability and behavioural anomalies. Hum. Genet. *137*, 401–411.
8. Kremer, L.S., Bader, D.M., Mertes, C., Kopajtich, R., Pichler, G., Iuso, A., Haack, T.B., Graf, E., Schwarzmayr, T., Terrile, C., et al. (2017). Genetic diagnosis of Mendelian disorders via RNA sequencing. Nat. Commun. *8*, 15824.
9. Wagner, M., Berutti, R., Lorenz-Depiereux, B., Graf, E., Eckstein, G., Mayr, J.A., Meitinger, T., Ahting, U., Prokisch, H., Strom, T.M., and Wortmann, S.B. (2019). Mitochondrial DNA mutation analysis from exome sequencing-A more holistic approach in diagnostics of suspected mitochondrial disease. J. Inherit. Metab. Dis. *42*, 909–917.
10. Alby, C., Boutaud, L., Bessières, B., Serre, V., Rio, M., Cormier-Daire, V., de Oliveira, J., Ichkou, A., Mouthon, L., Gordon, C.T., et al. (2018). Novel de novo ZBTB20 mutations in three cases with Primrose syndrome and constant corpus callosum anomalies. Am. J. Med. Genet. A. *176*, 1091–1098.
11. Sobreira, N., Schiettecatte, F., Valle, D., and Hamosh, A. (2015). GeneMatcher: a matching tool for connecting investigators with an interest in the same gene. Hum. Mutat. *36*, 928–930.
12. He, P., and Moran, G.R. (2011). Structural and mechanistic comparisons of the metal-binding members of the vicinal oxygen chelate (VOC) superfamily. J. Inorg. Biochem. *105*, 1259–1272.
13. Thul, P.J., Åkesson, L., Wiking, M., Mahdessian, D., Geladaki, A., Ait Blal, H., Alm, T., Asplund, A., Björk, L., Breckels, L.M., et al. (2017). A subcellular map of the human proteome. Science *356*, 356.
14. Calvo, S.E., Clauser, K.R., and Mootha, V.K. (2016). MitoCarta2.0: an updated inventory of mammalian mitochondrial proteins. Nucleic Acids Res. *44* (D1), D1251–D1257.
15. Claros, M.G., and Vincens, P. (1996). Computational method to predict mitochondrially imported proteins and their targeting sequences. Eur. J. Biochem. *241*, 779–786.
16. Valente, A.J., Maddalena, L.A., Robb, E.L., Moradi, F., and Stuart, J.A. (2017). A simple ImageJ macro tool for analyzing mitochondrial network morphology in mammalian cell culture. Acta Histochem. *119*, 315–326.
17. Haack, T.B., Jackson, C.B., Murayama, K., Kremer, L.S., Schaller, A., Kotzaeridou, U., de Vries, M.C., Schottmann, G., Santra, S., Büchner, B., et al. (2015). Deficiency of ECHS1 causes mitochondrial encephalopathy with cardiac involvement. Ann. Clin. Transl. Neurol. *2*, 492–509.

The American Journal of Human Genetics, Volume *107*

Supplemental Data

Bi-allelic *HPDL* Variants Cause a Neurodegenerative Disease Ranging from Neonatal Encephalopathy to Adolescent-Onset Spastic Paraplegia

Ralf A. Husain, Mona Grimmel, Matias Wagner, J. Christopher Hennings, Christian Marx, René G. Feichtinger, Abdelkrim Saadi, Kevin Rostásy, Florentine Radelfahr, Andrea Bevot, Marion Döbler-Neumann, Hans Hartmann, Laurence Colleaux, Isabell Cordts, Xenia Kobeleva, Hossein Darvish, Somayeh Bakhtiari, Michael C. Kruer, Arnaud Besse, Andy Cheuk-Him Ng, Diana Chiang, Francois Bolduc, Abbas Tafakhori, Shrikant Mane, Saghar Ghasemi Firouzabadi, Antje K. Huebner, Rebecca Buchert, Stefanie Beck-Woedl, Amelie J. Müller, Lucia Laugwitz, Thomas Nägele, Zhao-Qi Wang, Tim M. Strom, Marc Sturm, Thomas Meitinger, Thomas Klockgether, Olaf Riess, Thomas Klopstock, Ulrich Brandl, Christian A. Hübner, Marcus Deschauer, Johannes A. Mayr, Penelope E. Bonnen, Ingeborg Krägeloh-Mann, Saskia B. Wortmann, and Tobias B. Haack

Supplemental Data

SUPPLEMENTAL NOTE: CASE REPORTS

Family 1 (Congenital phenotype)

Individual F1:II.1 is an 8-year-old male, born to unrelated healthy parents from Algeria. His younger sister (F1:II.2) is similarly affected, a younger brother is healthy. IUGR was observed and he was born at term with a marked microcephaly (weight -3.2 SD, length -2.8 SD, head circumference -5.1 SD) and muscular hypotonia, and difficulty of sucking were noted. The further disease course was characterized by severely impaired psychomotor development, failure to thrive, and spastic movement disorder predominantly of the lower limbs. Generalized tonic-clonic seizures in the first year of life and motor partial seizures secondarily generalized at the age of 8 years were treated with valproic acid. MRI brain at the age of 7 years showed severe white matter reduction with parieto-occipital predominance, and very thin corpus callosum. Myelin signal was detectable throughout the white matter with diffuse signal increase on T_2-weighted scans affecting the periventricular region and U-fibres. Cerebellum appeared normal. Laboratory investigations, nerve conduction studies and electromyography were largely without pathologic findings. At the time of his last presentation at the age of 8 years key clinical features were severe intellectual disability and microcephaly, weak response to sensory stimulation, severe spastic movement disorder, axial dystonia, scoliosis, joint contractures of lower extremities, hips and elbows, growth retardation. Dysmorphological examination shows hypertelorism, long eyelashes, high-arched palate and anteverted nostrils. EEG showed slow background activity with epileptic abnormalities bilateral, diffusing to the whole left hemisphere.

Individual F1:II.2 is a 7-year-old female, born to unrelated healthy parents from Algeria. Her elder brother (F1:II.1) is similarly affected, a younger brother is healthy. She was born at term with normal birth weight (length and head circumference not documented) and displayed muscular hypotonia. Head circumference documented at the 3rd week of life was -4.4 SD, body length at the age of 6 month -6.1 SD. At the age of 2 months secondary generalized partial motor seizures and generalized tonic-clonic seizures occurred every 10 to 15 days and were treated with valproic acid. Examination at 2 years of age showed microcephaly (-4.1 SD), spastic movement disorder predominantly of the lower limbs, and axial dystonia. The child does not follow the light well and has a low visual acuity, does not react to the call by her name. Dysmorphological examination shows big wide-eyed, thick eyelashes, long lashes, hollowed philtrum, anteverted nostrils, prominent upper lips, retrognathism, high-arched palate and short neck. Development remains stationary, without new achievements. Examination at the age of 7 years showed severe intellectual disability without expressive speech, she was unable to eat alone, had a growth retardation with a weight of 15 kg (-2.7 SD), length 97 cm (-4.5 SD), head circumference 43.5 cm (-5 SD) as well as impaired vision, spastic movement disorder, mild scoliosis, and joint contractures (knee, ankle). EEG showed poorly organized, slow background activity with focal and generalized epileptiform activity. Blood lactate was normal (2 mmol/l; ref.

range 0.70- 2.10) and CSF lactate elevated at 6.20 mmol/l (ref. range 0.89-1.66 mmol/l). Brain MRI at the age of 5 years showed a severe white matter volume reduction with parieto-occipital predominance and a thin corpus callosum. Myelin signal (T_2-weighted scans) was seen in the optic radiation, inner capsule, to some extent in central white matter, but not in U-fibres. Cerebellum appeared normal.

Family 2 (Infantile phenotype)

Individuals F2:II.1 and F2:II.3 are children of healthy parents who are 1st degree cousins of Iranian descent. They are currently 34 respectively 21 years old. Both individuals were born after an uneventful pregnancy by vaginal delivery. None of them showed dysmorphic features at birth. Parents realized motor problems in infancy at about 6 months of age in F2:II.1 and at about 2 months of age in F2:II.3 with motor weakness. Regression occurred in both individuals from the age of 3 years onwards. Both showed poor feeding and failure to thrive (body weight not available). They furthermore developed microcephaly (-4.6 SD resp. -5.3 SD at 18 years of life), progressive tetraparesis with severe spasticity and they never became ambulatory. Joint contractures of hand and foots were observed and they did not develop expressive language. They had a history of generalized tonic clonic seizures but are currently without antiepileptic treatment. Electrophysiological testing including nerve conduction studies and electromyography showed normal results. Laboratory testing regarding neurometabolic disorders has not been performed. A difference observed in these two brothers was that the younger individual F2:II.3 had two episodes of apnea and he was hospitalized for mechanical ventilation in childhood. Brain MRI of F2:II.3 at the age of 19 years showed extreme global white matter volume reduction with very thin corpus callosum accordingly. Myelin signal (T_2-weighted scans) was seen in the subcortical white matter but not centrally. No myelin signal was detected in the optic radiation or inner capsule. Cortex not clearly affected and the cerebellum was mildly atrophic but with normal myelination.

Family 3 (Infantile phenotype)

Individual F3:II.3 is a boy and third child of healthy parents who are 1st degree cousins of Turkish descent. He was born at term after a normal pregnancy by cesarean section. His neonatal period was normal. In the following months, he showed a normal development. He was able to hold his head on traction. He was feeding well. At the age of five months, the parents noted abnormal posturing of his arms and he was seen by a neuropediatrician. An ultrasound examination of the brain revealed increased signal intensities of both thalami. At the age of six months he experienced an infection of the upper airways associated with fever and several neurological symptoms including an external ophthalmoplegia, significant truncal hypotonia combined with muscle weakness of all limbs and brisk deep tendon reflexes. He was admitted to a university hospital for further investigations. In the cerebral MRI marked signal hyperintensities in both thalami were confirmed (MRI images not available for review). Cerebrospinal fluid studies showed an elevated lactate of 2.74 mmol/l and alanine of 52 µmol/l (<39.5 µmol/l). A muscle biopsy examination including analysis of respiratory chain enzymes was performed revealing only unremarkable results. A repeat MRI scan of the brain 5 months later revealed a resolution of the signal intensities in both thalami (MRI images not available for review). Until the age of 2

years he developed a mild bilateral spasticity characterized by an increased muscle tone in particular of the lower limbs, increased deep tendon reflexes, and a positive Babinski's sign but age-appropriate cognitive skills. By the age of 2 years he was able to walk on his own. He was able to speak in short sentences with good language comprehension. At the age of 6 years his parents noted a mild decline of his motor skills without a preceding infection. He was only able to walk short distances and needed help to get up from the floor. At the age of 11 years he was still able to walk with a posterior gait walker and to ride a therapy bicycle. At that time his mother noted symptoms compatible with external ophtalmoplegia. Two months later he suffered from a viral throat infection which was followed by a dramatic worsening of his neurological condition with marked dysarthria and generalized weakness. He was admitted to a tertiary hospital. The neurological examination revealed an incomplete external ophthalmoplegia, truncal hypotonia, and profound muscular weakness. He was unable to stand or walk. His voice was very low-pitched and his speech dysarthric. In addition, he had three unprovoked tonic-clonic generalized seizures in one day. He further had an elevated blood pressure and an irregular breathing pattern characterized by very shallow and reduced frequency of breaths per minute with long interval combined with a marked hyperkapnia. At 11 years of age brain MRI (T_2-weighted scans) showed multifocal cortico-subcortical signal changes as well as diffuse signal changes of the thalamus, mediodorsal thalamic nuclei, periaquaeductal grey, and extensively in brain stem with involvement especially of olivae, also involving lower pons. A small lactate peak was observed in the parietal lobe without clear contrast enhancement or diffusion changes. Spinal cord scans showed mild central T_2-weighted signal hyperintensities, most pronounced in the cervical spine. CSF studies performed during this episode showed normal cell count, total protein, and lactate levels. CSF alanine was elevated with 34.2 µmol/l (range: 19.9-31.3 µmol/l). No intrathecal synthesis of IgG was detectable. Autoantibodies against neuronal antibodies such as NMDA-receptor were all negative. All aspects taken together an energy dependent metabolic disease was favoured but an autoimmune process could not be fully disregarded at the time. Therefore, high dose intravenous methylprednisolone therapy for three days was administered followed by a course of intravenous immunoglobulins. The cerebral MRI six days after the last study showed a significant improvement with T_2-weighted signal alteration being less prominent in all regions and a lactate peak in the parietal lobe. Despite the radiological improvement the boy developed a respiratory insufficiency with respiratory rate of 8/min and a markedly elevated CO_2 leading to admission to intensive care unit and subsequent mechanical ventilation. Pneumonia due to Mycoplasma pneumoniae was diagnosed. After four days he was extubated and recovered rapidly in the following days. Another brain MRI 13 days later showed further receding T_2-weighted signal changes, most prominent still in the brain stem, mediodorsal thalamus, and some cortical areas (mostly parietal left). He was discharged in stable condition and was referred to an in-house intensive rehabilitation program. MRI follow-up at the age of 11 5/12 years showed receding T_2-weighted signal changes in the brain stem, abnormalities especially in frontal areas (olivae) and a new bilateral pathology in the posterior part of the inferior colliculi. MRI at the age of 11 10/12 years showed brain stem abnormalities as described above; signal changes in posterior part of inferior colliculi bilaterally appeared to be more prominent and in addition swollen, but without clinical worsening.

Family 4 (Infantile phenotype)

Individual F4:II.1 is a 10-year-old male, born after normal pregnancy to healthy 1st degree cousins from Syria. He has three healthy younger siblings with one of them born preterm at 32 weeks of gestation. Another younger sister has clubfeet and finger contractures attributed to Xq11.2 duplication. A maternal uncle was reported to never have been ambulant without further explanation. Otherwise, the family history was unremarkable. The boy's development was initially unremarkable, with walking at the age of 1 year, normal speech development, continence in 2nd year of life and being able to run until about the age of 3 years. Then a developmental regression occurred with loss of ambulation at the age of 4 years and reduced active speech. Brain imaging at that point in the country of origin was reported to be without pathological findings (images not available for review). He developed a leg-dominated spastic motor disorder and showed a slow regression. Furthermore, intermittent nystagmus and pain at night were noted. After relocation to Germany, a neurodegenerative disease was suspected and diagnostics at the age of 7 years were initiated. Metabolic laboratory including lactate in CSF was unremarkable. Brain MRI showed on T_2-weighted and Flair images cerebellar white matter signal changes in subcortical areas with lateral predominance; signal hyperintensities were also seen in the central brain stem, as well as mediodorsal thalamic nuclei, superior and inferior colliculi and mildly cerebellar pedunculi. Wernicke encephalopathy was suspected. With low normal vitamin B12 blood level a single dose of vitamin B12 was administered. One month later at the age of 7 5/12 years, he suddenly developed lethargy and consecutive central respiratory failure requiring mechanical ventilation. An emergency cerebral CT scan was unremarkable. After transfer to university hospital brain MRI showed no clear pathology except suspected signal changes in the mediodorsal thalamic nuclei, MR-spectroscopy was not clearly abnormal. Extensive diagnostics were without pathological findings. CSF neurotransmitters showed slightly elevated homovanillic acid and 5-hydroxyindole acetic acid levels and low tetrahydrobiopterin, whereas urinary pterins were later to be found normal. A thiamine transporter-2 deficiency was suspected and treated with thiamine and biotin. After recovery from respiratory failure further developmental regression occurred. Follow-up MRI at the age of 8 2/12 years showed hyperintense T_2-weighted signal changes of the central cerebellar white matter and brain stem (olivae) as well as inferior colliculi. Spine appears normal, MRS with lactate peaks. Another MRI performed at the age of 8 3/12 years after head concussion displayed a more marked pathology with more extensive cerebellar white matter signal changes, changes in central anterior brain stem and swelling of inferior colliculi (extending to superior colliculi), here also suspected contrast enhancement. Electrophysiology studies eventually demonstrated severely reduced motor and slightly reduced sensory nerve conduction velocity. An abnormal variation in muscle fibre diameter was found. Biochemical investigations revealed complex I/IV-deficiency in muscle but not in fibroblasts. At the current age of 10 years, the boy shows leg-dominated spastic motor disorder with knee contractures, mild intellectual disability, speech disturbance, visual disturbance with convergent strabismus, incontinence, obese body stature with prediabetes and suspected lipoedema.

Family 5 (Infantile phenotype)

Individual F5:II.2 is a 22-year-old male with intellectual disability, motor impairments, and epilepsy born to unrelated parents from Canada. He had a younger brother who passed away at 6 weeks of age after rapidly deteriorating from an unknown illness. At day 4 of life, individual F5:II.2 developed feeding issues and experienced a 15 minute long seizure of unclear etiology. He experienced developmental delay of motor milestones and began showing spasticity in the lower limbs as well as truncal hypotonia. Development of language acquisition was also delayed and he has intellectual disability, which appears severe but was not formally tested. At age 2 years the individual had surgery to address esotropia in both eyes. Spasticity in the lower limbs progressed to the point that he required surgery at age 3 years to release adductors in both legs. One month post-surgery, the individual was admitted to the hospital for one hour long febrile status epilepticus. At age 4 years the individual had surgery to release both heels. MRI at the age of 5 years revealed a right mesial temporal spherical lesion (9 x 11 mm) that did not enhance with gadolinium. This lesion did not enlarge with subsequent MRIs. There was also generalized diminished volume of the white matter with thinning of corpus callosum. By age 9 years, his mobility continued to decline and he received frequent botulinum toxin injections. His EEG at age 12 years showed frequent focal and generalized epileptiform discharges, maximally in the bilateral frontocentral areas. The background was in the theta range, which was slow for age. By age 14 years, he could commando crawl and roll over. Brain MRI at age 14 years revealed a new T_2 hyperintense lesion in the left middle cerebellar peduncle measuring 11 mm. This lesion was also stable in size. The MRI of the whole spine was normal. Ultrasound of the abdomen revealed no gross organomegaly. A swallow study done at age 17 years showed silent aspiration. Repeat EEG at age 18 years showed slow background (theta range) but no epileptiform discharges were identified. Currently, at the age of 22 years, he has severe bilateral lower limb spasticity and ankle clonus with his left side worse than right. Deep tendon reflexes in the upper limbs were within normal limits. His head circumference was 56.5 cm (84 percentile). His weight was 84.5 kg (83 percentile) and length approximately 152 cm (-3 SD). His other medical conditions include restless leg syndrome. He speaks in 2-word sentences and can sign 30 words. His medications include carbamazepine, phenobarbital, gabapentin, baclofen, trazodone, and melatonin. Lactate was elevated in blood (4.3 mmol/l), further investigations into inborn errors of metabolism including plasma amino acid, urine organic acids, and ammonia were normal. Blood work for coagulopathy and immunoglobulins were normal. Genetic testing including chromosomal microarray, Rett syndrome, and Angelman syndrome were unremarkable.

Family 6 (Infantile phenotype)

Individual F6:II.1 is a currently 5-year-old boy born to unrelated parents from Germany. He has a healthy younger sister and a similarly affected younger brother (individual F6:II.3). Epilepsy was reported in the father's childhood and in a paternal uncle since adolescence, otherwise family history is unremarkable. After a normal pregnancy, the boy was born at term with microcephaly (33 cm, 4^{th} percentile). Excessive crying, muscular hypertonia and prolonged sleep duration were noted. At the age of 3 weeks cyanotic apneas led to hospitalization and extensive diagnostics after transfer to a university hospital. Lactate was elevated in blood (4.0 mmol/l,

normal range: 0.5-2.2 mmol/l) and CSF (6.9 mmol/l, normal range: 1.1-2.8 mmol/l), as was alanine in blood (501 µmol/l; normal range: <439 µmol/l) and CSF (91.1; normal range 13.8-32.6 µmol/l). Brain MRI showed dysgenesis of the corpus callosum and unilateral small punctiform lesions of the left basal ganglia with diffusion restriction. A few days later brain ultrasonography revealed increased echogenicity of the thalami and periventricular region interpreted as focal oedema. Apneas were interpreted as seizures without distinct EEG alterations and treated with phenobarbital and subsequently levetiracetam, leading to clinical stabilization. A small muscular ventricular septal defect was detected. Repeat brain MRI at 7 weeks of age showed little myelin signal on T_2-weighted scans (only posterior pons shows low signal), white matter appeared abnormally hyperintense but without diffusion changes. Focal T_2-weighted signal alterations were observed in the left caudate head and lateral ventricles were mildly enlarged. Corpus callosum appeared reduced in volume and a subsequent MRI at 15 months of age showed a reduction in the parieto-occipital white matter volume with enlargement of ventricles and a volume loss of the corpus callosum. Posterior limb of the internal capsule, optic radiation, central white matter, and splenium showed some myelin signal on T_2-weighted images. Myelination appeared normal infratentorially. In the further course progressive microcephaly (-3.25 SD), failure to thrive (-2.85 SD), growth retardation (-2.63 SD), global developmental delay, mild intellectual impairment, bilateral spasticity of the lower limbs, dysarthria, sialorrhoea, incontinence, hyperopic visual impairment, and nystagmus occurred. Surgical procedures regarding herniotomy, hydrocele testis and hip surgery were required. Currently he can crawl and pull himself into kneeling upright, uses his wheelchair actively, grasps, eat with his hands, drink through a straw, differentiate known and unknown persons, objects and situations, communicates by looking and gesturing, but cannot verbalize. Genetic diagnostics were unremarkable including chromosomal analysis, array-CGH and mitochondrial genes including Leigh syndrome-associated variants.

Individual F6:II.3 is a currently 1 7/12 years old boy and the brother of individual F6:II.1 (see above). Pregnancy was uneventful and he was born at term with normal weight, length and head circumference without any postnatal issues. Routine brain ultrasonography showed mild ventriculomegaly. He presented in the 2nd month of life with cyanotic apneas that led to hospitalization and transfer to university hospital. Ongoing apneas required intermittent non-invasive ventilation resp. nasal high flow treatment and medication with caffeine citrate. Laboratory diagnostics showed elevation of lactate in blood (7.9 mmol/l, normal range: 1.1-2.3 mmol/l) and CSF (8.2 mmol/l, normal range: <2.1 mmol/l) as well as alanine (blood 828 resp. CSF 73.6 µmol/l (normal range: 23.0-39.5 µmol/l). Urinary organic acids showed lactate, fumarate, malate elevated and pyruvate slightly elevated. Other metabolic investigations including acylcarnitines, neurotransmitters and FGF21 did not reveal significant changes. Brain MRI at the age of 6 weeks showed no myelin signal (T_1- and T_2-weighted images), enlarged ventricles, white matter signal appeared highly abnormal (T_2-weighted hyperintensities); anterior putamen and head of caudate bilaterally showed hyperintensity on T_2-weighted scans without diffusion changes; MR-spectroscopy revealed a clearly abnormal lactate signal in this region. Corpus callosum appeared reduced in volume. Due to these findings and family history a mitochondrial disease was suspected and vitamin-cofactor therapy was started with

ubidecarenone, biotine, thiamine and riboflavin. In polysomnography prolonged central apneas (duration >5.5 s: mean 17.3 s, maximal 67.5 s; 5.2 s n/h) were detected with preceding global spindle oscillations. Although EEG diagnostics were largely unremarkable recurring severe apneas were assumed to be seizure-related and treated with levetiracetam. Only after addition of topiramate apneas ceased. Elevation of lactate and alanine quickly normalized. Echocardiography showed a normal function with a slightly enlarged left ventricle (LVIDD 26 mm) and a prominent septal wall thickness (IVS 4-4.5 mm). Sucking weakness required feeding via naso-gastric tube. Three weeks after admission the individual was stable enough for discharge. At follow-up with 4 months of age parents reported excessive crying lasting shortly after discharge as well as ongoing seizures, feeding problems with regurgitation, sensitivity to stress and intermittently impaired visual function. Gain of body weight, length and head growth was inadequate leading to secondary microcephaly (38 cm; -2.61 SD). Overall neurologic development was not adequate with muscle stiffness, clenched fists, tendency to opisthotonic posturing. EEG showed mulitfocal spikes bifrontally. Follow-up at 7 months of age showed developmental progress, unchanged EEG alterations, no lactate elevation in blood, urine and CSF and fewer central apneas in sleep study. MRI brain showed significant white matter volume reduction and ventricular enlargement with predominance parieto-occipital and significant volume loss of corpus callosum. Posterior limb of the internal capsule (PLIC) and optic radiation showed some myelin signal on T_2-weighted images, cerebellar white matter was myelinated. Basal ganglia appeared normal without clear signs of signal alteration or atrophy. Muscle biopsy did not show histopathologic changes. Enzymatic analysis of mitochondrial respiratory chain complexes showed marginally reduced complex I and reduced complex IV activitiy in snap-frozen muscle specimen and complex II, III, IV and V activities above upper limit in fibroblasts. No further episodes of metabolic decompensation occured and medication was stepwise reduced to levetiracetam and ubidecarenon only. At the last follow-up at 19 months of age microcephaly was more pronounced (43.7 cm; -4.2 SD), axial hypotonia and increased muscular tone with spasticity of predominantly the legs were present, feeding problems partly persisted. Munich Functional Developmental Diagnostics (MFDD) showed the following developmental ages: crawling 3 months, sitting 4-6 months, walking 5 months, gripping 5-6 months, speaking 3-4 months, perception 5 months, social skills 6 months. Seizures with fencing reflex-like movements occurred daily in clusters, EEG showed multifocal spikes and spike-waves predominantly in the temporal and focal regions, leading to additional treatment with oxcarbazepine.

Family 7 (Infantile phenotype)

Individual F7:II.2 is a boy and the second of three children of German ancestry. An older and a younger sister as well as both parents do not have any health concerns. During pregnancy, the mother felt less child movements in comparison with her other pregnancies. Due to breech position, he was born by caesarean section in the 39th week of gestation. Birth weight was normal, head circumference 40 cm (+3.4 SD), APGAR scores 9-10-10 and he had an uncomplicated adaptation and neonatal course. At the age of 6 weeks his parents observed short episodes with decreased consciousness followed by short uncontrolled movements while breastfeeding. EEG determined that these were epileptic seizures and he was treated with

phenobarbital and levetiracetam. CSF lactate was mildly elevated 3.8 mmol/l (no serum lactate levels available), plasma amino acids showed mildly elevated serine and citrulline and CSF amino acids showed mildly elevated alanine and methionine. Urinary organic acids and acylcarnitines in dried blood spot as well as CSF neurotransmitters were unremarkable. Brain MRI at the age of 2 months showed no myelin signal (T_1- and T_2-weighted), white matter signal appeared highly abnormal, especially in the frontal area (T_2-weighted hyperintensities); putamen and head of caudate bilaterally appeared swollen and showed hyperintensity on T_2-weighted scans without diffusion changes. Corpus callosum was somewhat reduced in volume. Investigation of a muscle biopsy showed mild fibre type disproportion and possibly enlarged mitochondria, staining for NADH, COS, Cox-SDH and Gomori-Triochrom was unremarkable. Investigation of the respiratory chain enzymes (I, I+II, II, II+II, IV, V, PDHc) was unremarkable in fresh muscle, some of the substrate oxidation rates showed mild changes without a clear pathogenic pattern. Investigation of the respiratory chain enzymes in fibroblasts showed activities of complex I-IV above the upper limit. Since then no more seizures occurred and phenobarbital was stopped after 6 months and levetiracetam after 18 months. Brain MRI at the age of 12 months showed no significant white matter volume reduction or ventricular enlargement. Myelination was delayed, only PLIC and optic radiation showed some myelin signal on T_2-weighted images, cerebellar white matter myelinated. Basal ganglia appeared normal without clear signs of signal alteration or atrophy. The boy showed a delayed development, he learned crawling by the age of about 3 years and pulled himself to standing since the age of 2 6/12 years. At the age of 4 years he showed growth retardation with a length of 92 cm (-2.7 SD), weight 13 kg (-2.0 SD), and was microcephalic (-2.5 SD). He is currently aged 5 years and cannot sit or stand independently, but can move himself around in a wheelchair or with a walker. He cannot speak words and is currently learning to communicate with gestures. The parents report a very slow gaining of motor and verbal skills but no regression. The physical examination at the same age shows a friendly and cooperative boy, interacting with his parents and the examiner. He has a long philtrum and low implanted ears. He shows severe axial hypotonia with good head control. The muscle tone of the upper limbs is mildly elevated with elbow contractures; the muscle tone of the lower limbs is clearly increased with pes equinus. He has decreased facial expression, shows intermittend esotropia and an open mouth with continuous drooling. Compound-heterozygosity of the detected *HPDL* variants was apparent from the exome data due to close proximity of the variants with sequencing reads showing either one or the other change. Carrier testing showed that the change on the paternal allele occurred *de novo*.

Family 8 (Infantile phenotype)

Individual F8:II.1 is a currently 2 3/12-year-old boy born after normal pregnancy per caesarean section (malposition) and postnatal adaption was unremarkable. He is the first child of healthy unrelated parents from Germany. The mother had had two spontaneous abortions (each at 16 weeks of gestational age, the first diagnosed as heterotaxia, heart defect; the second as partial trisomy 21). Birth measurements were within normal range (length 54 cm, head circumference 34 cm, birth weight 4150 g). At the age of 5 months, a delay in motor development was noticed and neurological examination revealed truncal hypotonia and increased tendon reflexes. Brain

MRI showed multifocal and confluent signal changes bilaterally (hyperintensities on T_2-weighted scans and with some moderate ADC decrease) of basal ganglia (nucleus caudatus and putamen); myelination low normal (optic radiation, PLIC, central white matter, cerebellar white matter showed low T_2-weighted signal). Laboratory testing was normal apart from increased lactate concentrations in plasma (4.3 mmol/l, normal range: <2 mmol/L) and cerebrospinal fluid (CSF; 3.3 mmol/L, normal range: <2 mmol/L). At the age of 7 months, he developed an intermittent strabismus divergens but made otherwise good developmental progress. At the age of 13 months, he still had limited motor control of head and trunk. Brain MRI showed no new lesions, good progress in myelination and consolidation of the formerly detected lesions (only minor signal changes in caudate and putamen, no significant atrophy). There was no sign of increased lactate in spectroscopy and concentrations were normal in plasma and CSF. Biochemical analysis of a skeletal muscle specimen showed normal function of isolated mitochondrial respiratory chain complexes and PDHc, but a globally reduced mitochondrial respiration indicating a possible defect in cofactor metabolism or dysfunction of the mitochondrial membrane. Histological workup showed no ragged red fibers or COX-negative fibers but an abnormal variation in muscle fiber diameter compatible with motor neuron impairment. Supplementation with biotin, coenzyme Q and thiamine was started at the age of 13 months. At last examination, the individual showed good overall developmental progress, but an increasing spasticity of the lower limbs. On follow-up at age 2 3/12 years, he displayed low body weight (9.8 kg; -2.6 SD), low length (79 cm; -3.14 SD) and low head circumference (47.2 cm; -2.2 SD) but had made developmental progress without deterioration during infections. He grasped, crawled, vocalized and understood simple language. He showed leg dominated spasticity with increased tendon reflexes.

Family 9 (Infantile phenotype)

Individual F9:II.1, a currently 8-year-old girl, is the first child of healthy unrelated parents from Germany. Pregnancy and postnatal adaption were normal. She reached motor and cognitive milestones in time and walked without aid at 12 months of age. She was an active child and regularly took part in track and field training. At age 5 years, she started complaining about sore legs after exercise. At age 5 2/12 years, her gait became unsteady and parents sought medical advice. Clinical examination revealed increased muscle tone and tendon reflexes of the legs, with a positive Babinski sign. Eye movements and neurological exam of the arms were normal, there was neither ataxia nor dystonia. Cranial MRI was normal, spinal MRI was first reported as possibly abnormal with suspicion of long extended central signal changes (T_2-weighted) of the spinal cord. In view of this finding, she was started on prednisolone without improvement. A control MRI two weeks later was normal and in retrospect the possible abnormalities on the first MRI were interpreted as pulse artefacts. CSF cell count was 1/µl, CSF protein 0.19 g/l, CSF lactate 2.36 mmol/l (normal range: 1.1-1.9 mmol/l). Plasma aminoacids were normal as were lactate and pyruvate in serum and both liver and kidney function tests. Treatment with L-dopa did not lead to a definite improvement. At age 6 6/12 years she lost free ambulation and neurogenic bladder dysfunction was noted. Genetic testing revealed a heterogeneous stop variant of the *SLC52A3*. Since recessive-type *SLC52A3* variants lead to Brown-Vialetto-van Laere syndrome, a trial with riboflavin supplementation was performed at age the age of 7 years

over a period of 6 months (2 x 100 mg per day) which had no clinical effect. Up from the age of 8 years, fine motor function of her upper limbs deteriorated and dysarthria was observed. Parents also noted learning difficulties. Currently, at an age of 8 5/12 years, she attends a special needs school and needs a writing aid.

Family 10 (Juvenile phenotype)

Individual F10:II.1 is a male born after unremarkable pregnancy and delivery to unrelated parents from USA. He had normal pediatric development and cognition. At the age of 15 years he came to clinical attention for back pain after increased exercise and unsteady gait. MRI of the brain was reported normal (MRI imaging not available for review). At most recent clinical evaluation, the individual was aged 17 years and had experienced progression of gait disturbance and stiffness. No other system involvement was reported. The individual was given a diagnosis of presumed hereditary spastic paraplegia.

Family 11 (Juvenile phenotype)

Individual F11:II.1 is a currently 20-year-old female. Her parents are 1st degree cousins from Turkey. The father suffers from myalgia, with muscle cramps and CK-elevation, but without spasticity. Similar muscular symptoms were also reported for the father's brother and sister, as well as his mother and her brother. The affected individual was born at term after normal pregnancy with neonatal jaundice requiring phototherapy. According to the parents all developmental milestones were reached, only a mild inward rotation of the left leg was observed from the age of 2 years on. Running and cycling was possible until teenage years. The woman reported on the onset of gait disturbances at the age of 15 years with progressive spasticity and paraparesis. Muscle cramping and myalgia limited the maximum walking duration to about 5 minutes. The maximum walking distance without pause is reduced to below 500 m. Moreover, she complained about intermittent paraesthesia of the calves. Occasional dysphagia without dysarthria and impaired short-term memory with attention deficits were reported. She did not take any regular medication apart from vitamin B12 and D supplements. At the age of 13 years an endocrine examination of sexual hormone levels was performed to clarify irregular menstrual cycles. The LH/FSH quotient was shifted, estradiol was slightly reduced, dihydrotestosterone was elevated. However, treatment was not initiated. Menstrual cycles are still irregular. The woman graduated from secondary school and is now in training for office management. Clinical examination revealed paraparesis with spasticity and increased reflexes in the lower limbs and weak reflexes in the upper limbs with a positive Babinski sign. A mild gait ataxia was observed but no signs of fine motor or sensory impairment. In addition, a syndactyly of the second and third toe on both feet up to the first interphalangeal joints, as well as a slightly abnormal position of the proximal phalanges of the index fingers were observed. The woman showed an obese body stature with a BMI of 34.9 kg/m² and suspected hirsutism. Functional testing resulted in SARA 6/40, ICARS 14/100, SPRS 10/52. Laboratory tests showed a slight elevation of CK 4.1 µkat/l (<2.8), myoglobin 69 ng/ml (25-58) and homocysteine 18.5 µmol/l (<12.0). Lumbar puncture was not performed. MRI imaging of the brain and spine showed no clear pathology. Nerve conduction studies and EMG revealed no abnormalities.

Family 12 (Juvenile phenotype)

Individual F12:II.3, a male, was the third child of healthy 1st degree cousins of Syrian origin. He had four healthy siblings. Development in childhood was normal up to the age of 15 years when gait disturbances became evident. Neurological examination revealed brisk reflexes of the arms and increased reflexes of the legs with a positive Babinski sign bilaterally. There was a bilateral spastic paresis of the legs with proximal predominance MRC (Medical Research Council) grade 3-4/5. Sensory functions and bladder function were normal. MRI examinations showed brain and spinal cord without signal alterations or malformations. CSF examinations were unremarkable. In the following years spastic paraparesis was progressive thus the individual was not able to walk independently any more at age of 19 years. However, no weakness of the arms occurred. At age of 19 years the individual presented at our university hospital for the first time. Medical history was compatible with pure hereditary spastic paraplegia with a possible autosomal recessive mode of inheritance.

Family 13 (Juvenile phenotype)

Individual F13:II.1 is a currently 39-year-old male and the first child of non-consanguineous parents from Turkey (near the Syrian border). He has two other siblings, one of whom (F13:II.2) is affected as well. The individual's medical history shows myopia and gastrointestinal reflux. A brain MRI was performed in adolescence as part of the diagnostic work-up of his walking problems and as an incidental finding a pituitary adenoma was diagnosed. It was removed transnasally a few years later because it was progressive in size. Similar to his brother, he had a normal development in childhood and was very active during his early adolescence. At the age of 14 years he had a period of immobilization due to an operation of a clavicular fracture. He then noticed for the first time a slowly progressive weakness of his left leg as well as fatigue. Later there was also slowly progressive paraspasticity, accompanied by muscle cramps and gait instability. Additionally he complained of a deterioration of the paraparesis after a walking distance of 2-3 km. Recently he noticed a mild bladder urgency. At his last presentation at the age of 28 years he showed a paraparesis and paraspasticity of the legs, increased reflexes of the legs and a spastic-atactic gait, suggestive of a pure hereditary spastic paraplegia phenotype, spastic paraplegia rating scale (SPRS) 7. Genetic testing of SPG4 and SPG7 were negative.

Individual F13:II.2 is a currently 33-year-old male and the second child in family 13. He has a healthy 3-year-old daughter. He reported a normal development in childhood and was reportedly physically very active during adolescence. At the age of 15 years during a period of increased physical activity during a soccer game he experienced a sudden “blockage” of his muscles accompanied by spasticity and paraparesis. Since then chronic-progressive deterioration of spasticity and gait instability without any sudden deterioration were observed. He also complained of recurrent muscle cramps and lumboischialgia. Physical examination at the age of 22 years showed a paraspasticity and a spastic-ataxic gait with increased reflexes of the legs. Spastic paraplegia rating scale (SPRS) was 17. Nerve conduction studies revealed no abnormalities, but delayed motor-evoked potentials were found. Medical history was suggestive of pure hereditary spastic paraplegia with an autosomal recessive mode of inheritance. Testing of HSP-related genes (SPG 5a, 7, 11) was negative.

SUPPLEMENTAL FIGURES AND LEGENDS

Figure S1

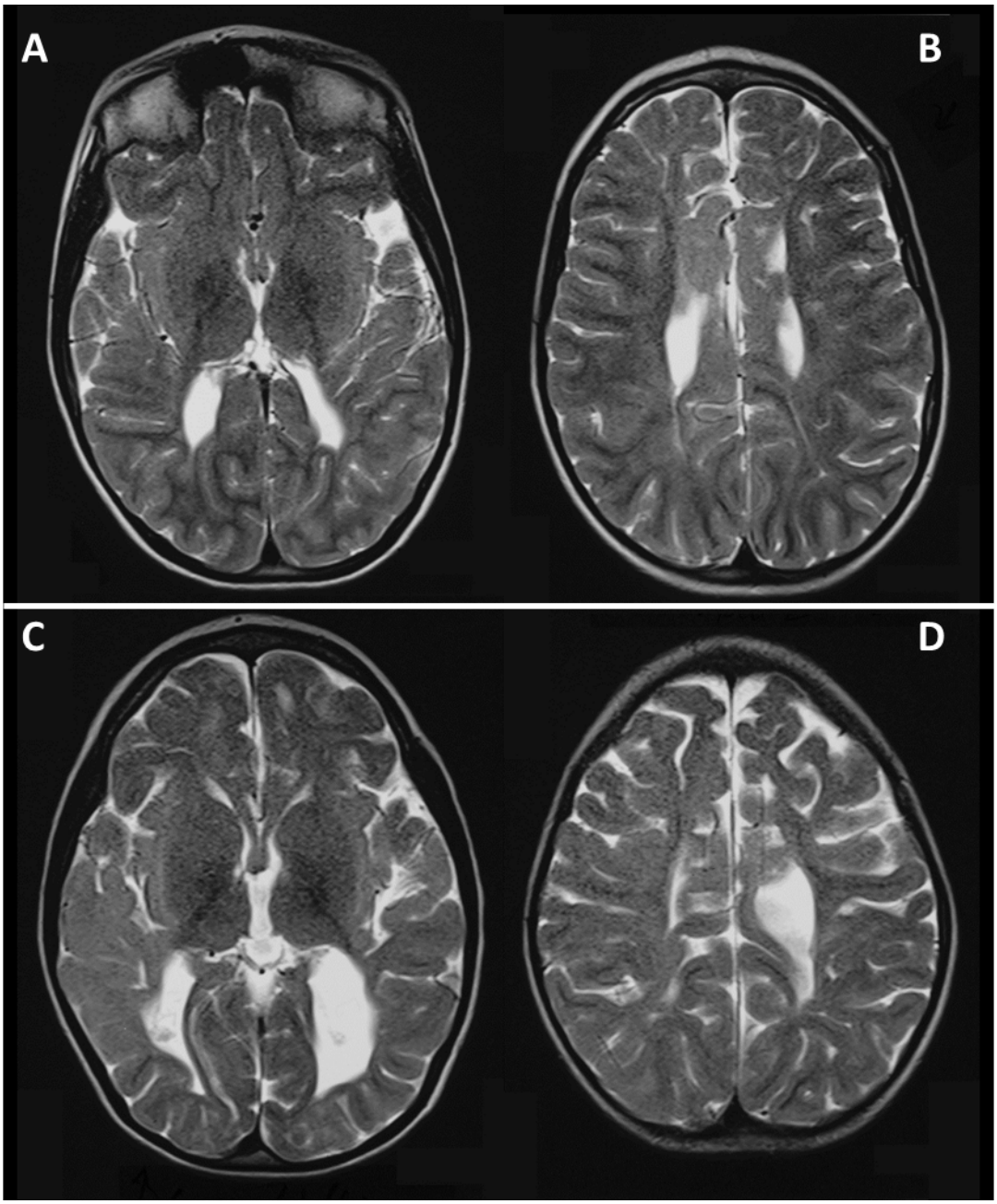

Figure S1. MRI Pattern I Suspected.

MRI (T_2-weighted axial scans) from individuals F1:II.1 (aged 7 years, A, B) and F1:II.2 (aged 5 years, C, D) show severe white matter volume reduction with parieto-occipital predominance. Accordingly the lateral ventricles are of irregular shape and the corpus callosum is very thin. Myelin signal of white matter shows diffuse signal increase concerning periventricular region and U-fibres. Summary of both individuals: White matter volume reduction suspicious of atrophy, myelination delayed.

Figure S2

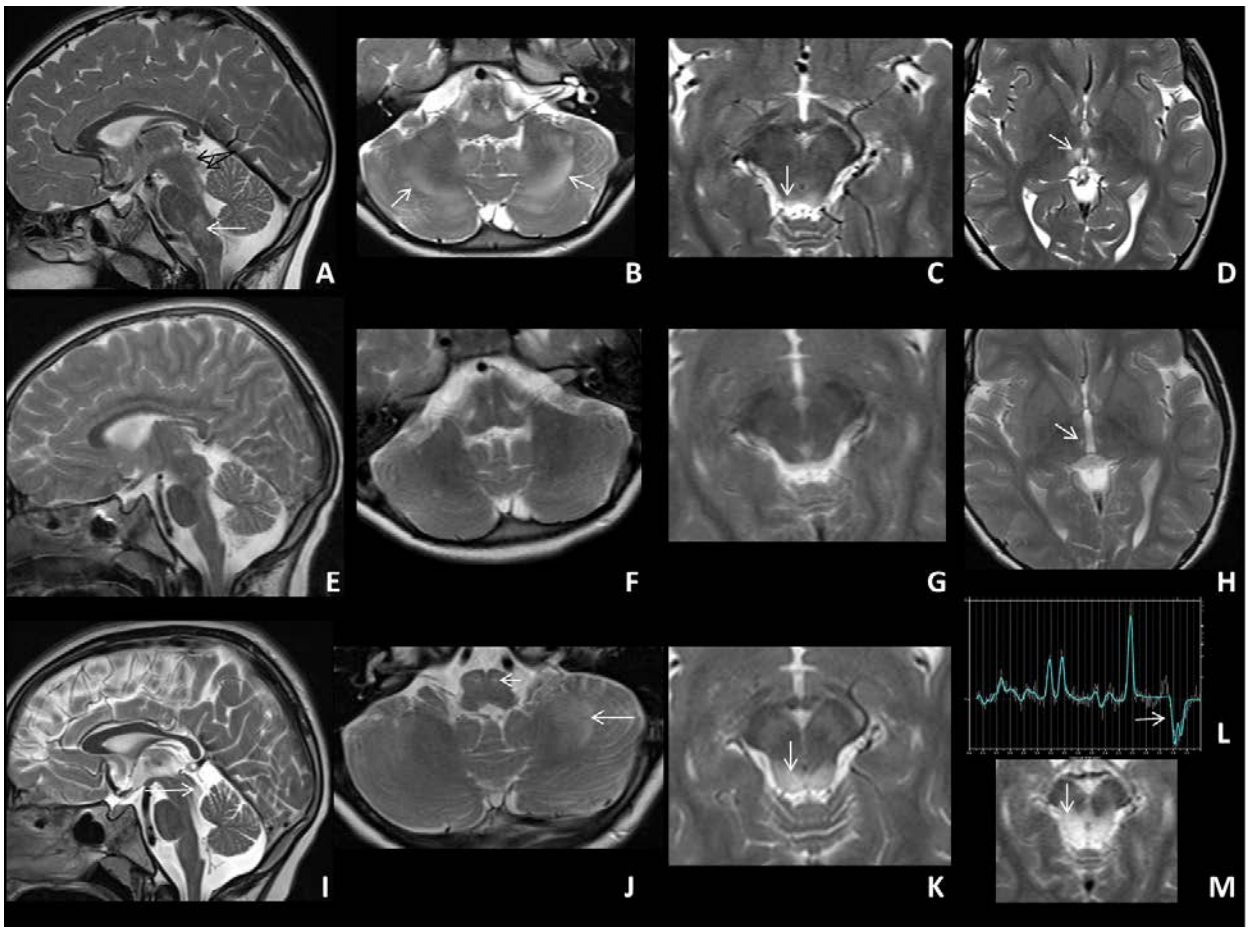

Figure S2. MRI Pattern II (continued from Figure 4).
MRI (T_2-weighted sagittal and axial scans) and MRS from individual F4:II.1
At the age of 7 4/12 years (A - D) signal hyperintensities are seen in the brain stem centrally (white arrow in A) and in the cerebellar white matter in subcortical areas with lateral predominance (white arrows in B). Superior and inferior colliculi show mild signal changes (black arrows in A, arrow in C). Mediodorsal thalamic nuclei show clear signal changes (arrow in D).
One month later at the age of 7 5/12 years (E - H) no clear pathology is evident except suspected signal changes in the mediodorsal thalamic nuclei (arrow in H).
At the age of 8 2/12 years (I - L), hyperintense signal changes are evident in the inferior colliculi (arrows in I, K). The central cerebellar white matter again is mildly hyperintense (arrow in J), as are the olivae (small arrow in J). Two months later, inferior colliculi appear even more hyperintense and swollen (arrow in M).
Summary: relapsing remitting course with initial changes in cerebellar white matter, mediodorsal thalamic nuclei, superior and inferior colliculi, showing remission, but relapsing with swelling of the inferior colliculi and additional brain stem changes.

Figure S3

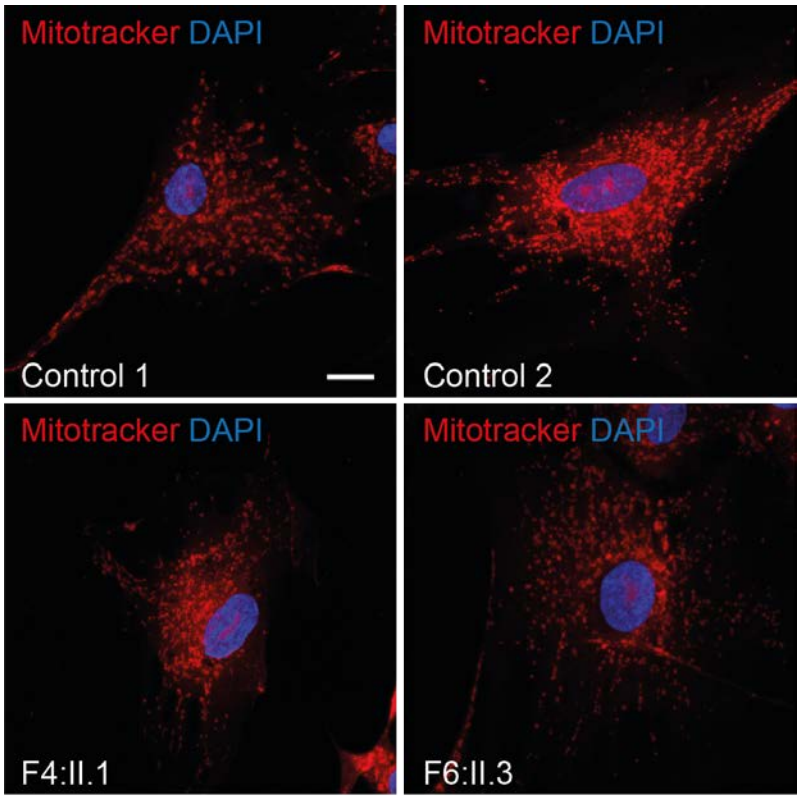

Figure S3. Investigation of Mitochondrial Morphology.

Analysis of the mitochondrial network visualized by Mitotracker Red CMXRos staining in fibroblasts from affected individuals and controls did not show significant differences. Fibroblasts from individuals (F4:II.1, F6:II.3) and controls (n=2) were grown on coverslips to near-confluency, incubated with 100 nM Mitotracker Red CMXRos (Invitrogen) in medium for 45 minutes at 37 °C and fixed with methanol at -20 °C for 15 minutes. DAPI staining (Invitrogen) was performed according to the instructions of the manufacturer. Fixed cells were mounted with Fluoromount G (Southern Biotech) and were analyzed with a Zeiss LSM 880 confocal microscope. Scale bar = 20 µm.

Figure S4

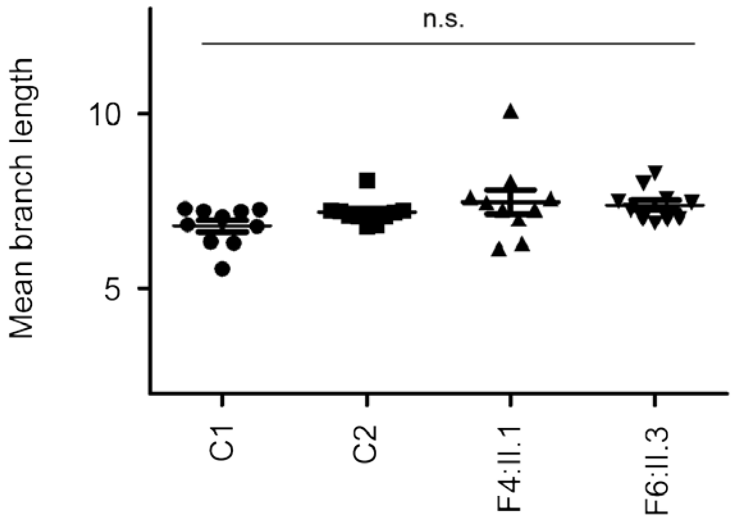

Figure S4. Analysis of Mean Mitochondrial Branch Length.

Analysis of the mitochondrial morphology using mean branch length as a parameter did not show significant differences between fibroblasts from affected individuals and controls. Methods see Figure S3. Mitochondrial morphology was analyzed with Fiji[2] using the Mitochondrial Network Analysis Tool (MiNA).[5; 6] n = 10 replicates per sample.

Figure S5

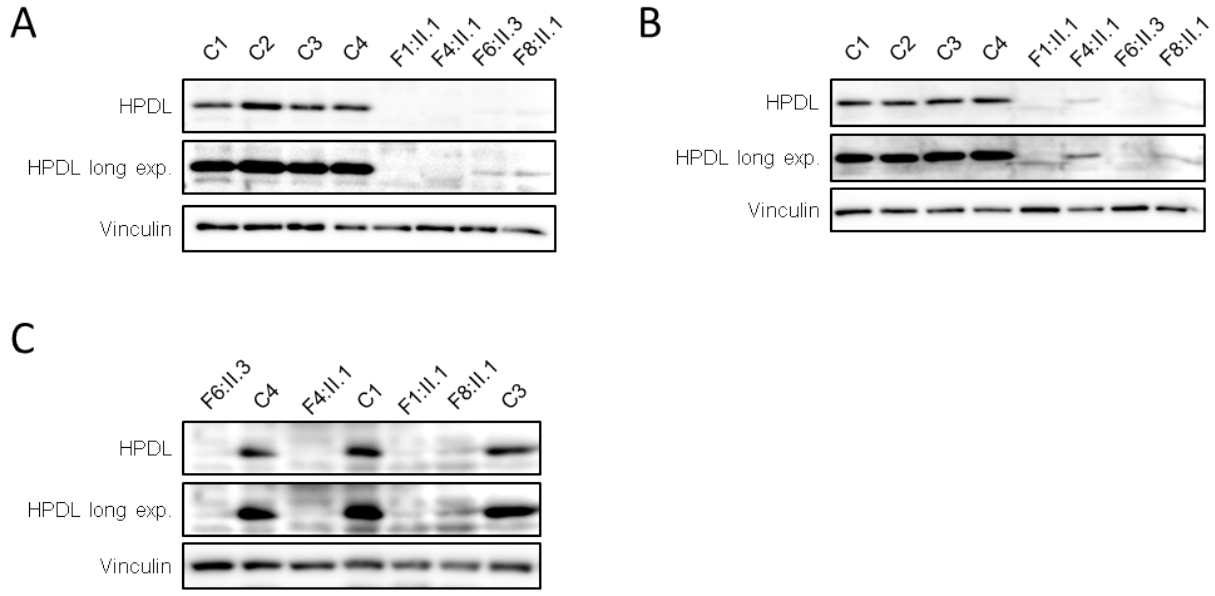

Figure S5. Relative HPDL Levels in Fibroblasts of HPDL-Deficient Affected Individuals Compared to Controls.

Whole cell lysates from fibroblasts of affected individuals (F1:II.1, F4:II.1, F6:II.3, F8:II.1; n=4) and controls (n=3 resp. n=4): After harvesting by scraping, cells were re-suspended in RIPA buffer (50 mM Tris/HCl (pH 8.0), 150 mM NaCl, 1 mM EDTA, 1 % Triton X-100, 1 % sodium deoxycholate and 0.1 % SDS) supplemented with PhosphoStop (Roche) and protease inhibitor cocktail (Roche), followed by brief sonication in a Bioruptor (Diagenode) (5 cycles with 30 s on and 30 s off with high intensity at 4 °C). Protein quantification was done with the Pierce BCA Protein Assay Kit (Thermo Fisher). Immunoblotting: All samples were diluted 5:1 in 6 x SDS-sample buffer (35 % β-mercaptoethanol, 350 mM Tris/HCl pH 6.8, 30 % glycerol, 10 % SDS, 0.25 % bromophenol blue) and heated at 95 °C for 7 min. 25 mg of protein per lane were separated by standard SDS-PAGE on polyacrylamide gels and transferred onto PVDF membranes. After blocking in blocking solution (BS; TBS pH 7.25, 5 % dry milk and 0.05 % Tween-20), membranes were incubated with primary antibody against HPDL (1:1000 diluted in BS; Proteintech). Equal loading of protein was verified by the detection of Vinculin (1:5000; Santa Cruz). Peroxidase-conjugated anti-rabbit (1:5000; KPL SeraCare) secondary antibody (diluted in BS) was used for detection of specific signals with Pierce ECL Western Blotting Substrate (Thermo Fisher) and Western Bright Sirius HRP substrate (Advansta) on an Amersham Imager 600 (GE Healthcare Lifesciences). Three independent experiments (A – C) were performed. The immunoblot of HPDL is displayed at normal exposure and overexposed (long exposure (exp.)) to show remaining HPDL levels in HPDL-deficient affected individuals' fibroblasts. Figure S5 panel A shows parts of Figure 2 panel A for better comparability.

Figure S6

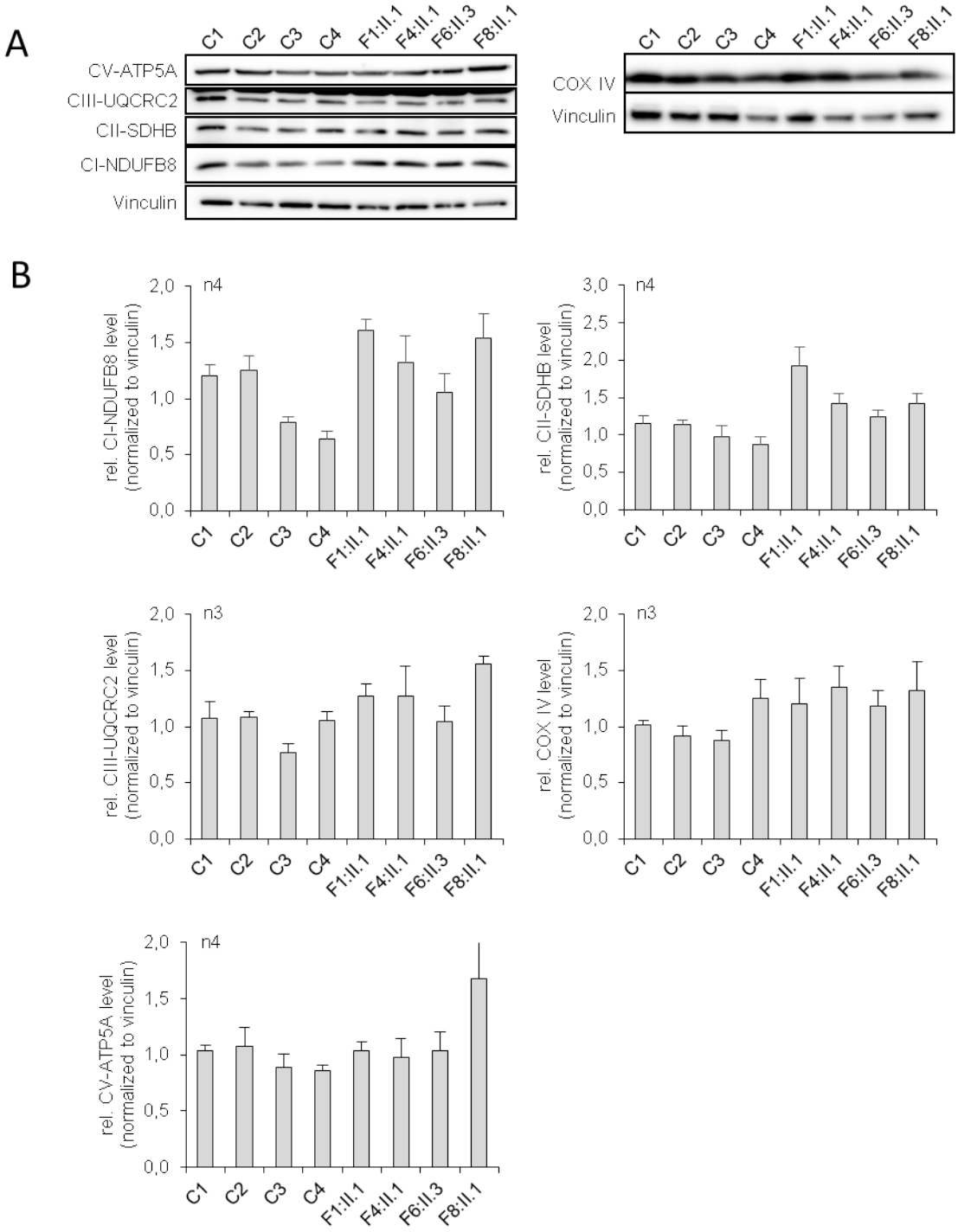

Figure S6. Relative Protein Levels of OXPHOS Complex Subunits in Fibroblasts of HPDL-Deficient Affected Individuals Compared to Controls.

(A) Whole cell lysates from fibroblasts of affected individuals (F1:II.1, F4:II.1, F6:II.3, F8:II.1; n=4) and controls (n=4) were prepared and analyzed by SDS-PAGE and immunoblot as described in Figure S5. Membranes were incubated with primary antibodies against total OXPHOS rodent WB antibody cocktail (complex V subunit ATP5A, complex I subunit NDUFB8, complex III subunit UQCRC2, complex II subunit SDHB, 1:2500 diluted in BS; Abcam), complex IV subunit COX IV (1:5000 diluted in BS; Abcam). Equal loading of protein was verified by the detection of Vinculin. Peroxidase-conjugated anti-mouse (1:5000 diluted in BS; KPL SeraCare) secondary antibodies were used for detection of specific.
(B) Protein levels were quantified using ImageJ (NIH). The graphs display the average of 3-4 individual experiments (n3, n4) ± SEM.

Figure S7

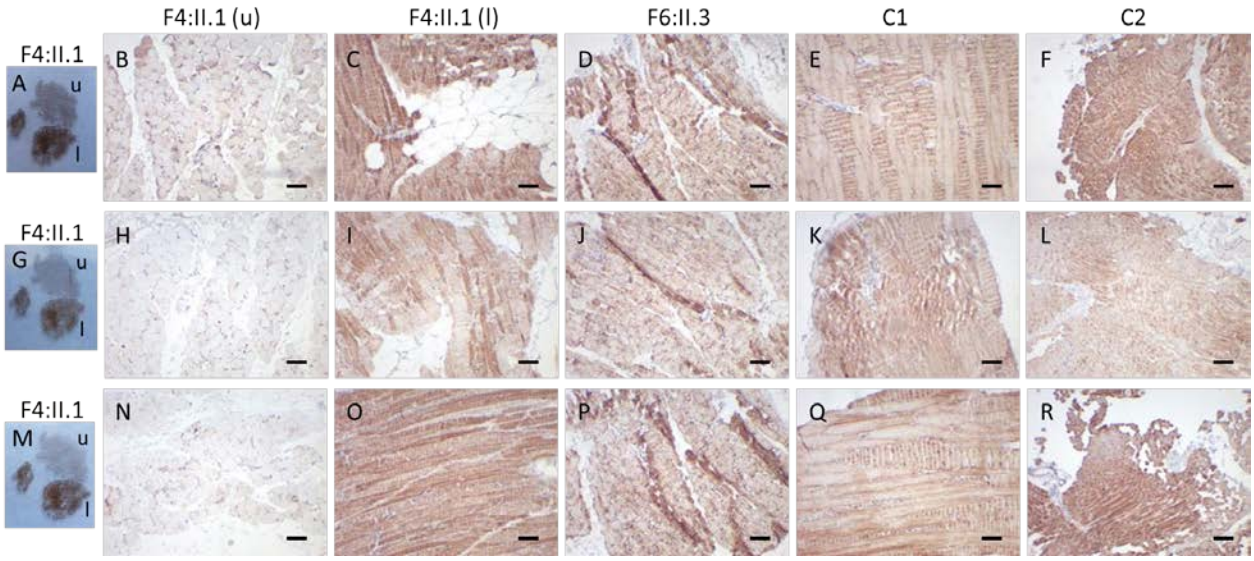

Figure S7. Immunohistochemical Staining of VDAC1, SDHA and MT-CO1 in Muscle Tissue of Two HPDL-Deficient Individuals (F4:II.1, F6:II.3) and Controls

Immunohistochemical staining of SDHA, MTCO1 and VDAC1 of formalin-fixed paraffin-embedded muscle tissues. (A-F): VDAC1 staining. (G-L): SDHA staining. (M-R): MT-CO1 staining. (A, G, M): Overview of the sample showing 3 muscle fibre bundles. (B, H, N): VDAC1, SDHA, MT-CO1 negative muscle fibre bundle of individual F4:II.1 upper (u) part of A, G, M respectively. (C, I, O): VDAC1, SDHA, MT-CO1 positive muscle fibre bundle of individual F4:II.1 lower (l) part of A, G, M respectively. Slides were stained with antibodies against complex II subunit SDHA (mouse monoclonal, 1:2000; Abcam), complex IV subunit MT-CO1 (mouse monoclonal, 1:1000; Abcam), and VDAC1 (mouse monoclonal, 1:2000; Abcam). All antibodies were diluted in antibody diluent with background-reducing components (Dako). IHC was performed as described previously.[7] Scale bar = 100 µm.

Figure S8

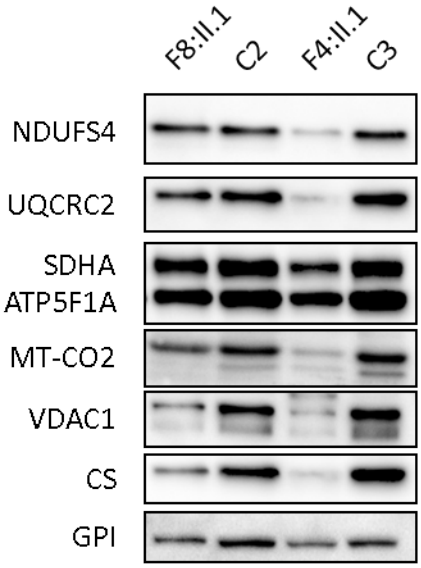

Figure S8. Relative Levels of OXPHOS Complex Subunits in Muscle Tissue Homogenate Are Reduced in One of Two Affected Individuals

A total of 10 µg protein of muscle tissue homogenate from affected individuals (F8:II.1, F4:II.1) and controls (n=2) (centrifuged at 600 g) was separated on 10 % acrylamide/bisacrylamide gels and transferred to nitrocellulose membranes. The membranes were washed in Tris-buffered saline (TBS) for 5 min, air-dried for 30 min, washed 10 min in TBS, and blocked 1 h at room temperature in 2 % blocking powder (Roche, Mannheim, Germany) dissolved in TBS. After washing with TBS-Tween 20 (0.5 %; TBS-T), the membranes were incubated with the primary antibody diluted in 2 % blocking powder dissolved in TBS-T. The following primary antibody dilutions and incubation times were used: monoclonal mouse NDUFS4 (1:1,000, 1 h, room temperature; Abcam), SDHA (1:2000, 1 h, room temperature; Abcam), UQCRC2 (1:1500, 1 h, room temperature; Abcam); MT-CO2 (1:1000, 1 h, room temperature; Abcam), ATP5F1A (1:2000, 1 h, room temperature; Abcam), VDAC1 (1:2000, 1 h, room temperature; Abcam), CS (1:3000, 1 h, room temperature; THP), GPI (1:800, 1 h, room temperature; Santa Cruz). After washing, the membranes were incubated with secondary antibodies labeled polymer horseradish peroxidase-(HRP)-antimouse 1:1,00 (EnVision kit, Dako) at room temperature. Detection was carried out with Lumi-LightPLUSPOD substrate (Roche).

SUPPLEMENTAL TABLES

Table S1

	Enzyme activities [nmol/min/mg protein]					
Individual	Citrate synthase	Complex I	Complex II	Complex III	Complex IV	Complex V
F4:II.1	86	2	15	74	37	27
F6:II.3	197	17	267	148	67	114
Control, lower limit	*134*	*18*	*28*	*149*	*148*	*60*
Control, upper limit	*260*	*59*	*69*	*480*	*392*	*223*
Specimen: frozen muscle						
F7:II.2	214	48	58	803	472	167
F8:II.1	196	34	55	654	396	184
Control, lower limit	*150*	*28*	*33*	*304*	*202*	*86*
Control, upper limit	*338*	*76*	*102*	*896*	*889*	*257*
Specimen: native muscle						

Table S1. OXPHOS Enzymes in HPDL Muscle Mitochondria Were Variably Reduced in Two Affected Individuals.

Primary biochemical data of individual F3:II.3 was not available for review but enzymatic activities were rated as normal according to the provided clinical information. In the remaining individuals, enzyme activities of the OXPHOS complexes were determined as previously described.[1] Briefly, rotenone-sensitive complex I activity was measured spectrophotometrically as NADH/decylubiquinone oxidoreductase at 340 nm. The enzyme activities of citrate synthase and complex IV (ferrocytochrome c/oxygen oxidoreductase), and the oligomycin-sensitive ATPase activity of the F_1F_O ATP synthase (complex V) were determined by using buffer conditions as previously described.[2] The whole reaction mixture for the ATPase activity measurement was treated for 10 s with an ultra-sonifier (Bio cell disruptor 250, Branson, Vienna, Austria). The reaction mixture for the measurement of the complex III activity contained 50 mM potassium phosphate buffer pH 7.8, 2 mM EDTA, 0.3 mM KCN, 100 µM cytochrome c, 200 µM reduced decyl-ubiquinol. The reaction was started by addition of the 600 g homogenate. After 3-4 min the reaction was inhibited by addition of 1 µM antimycin A. Antimycin A-insensitive activity was subtracted from total activity to calculate complex III activity. All spectrophotometric measurements (Uvicon 922, Kontron, Milan, Italy) were performed at 37 °C.

Table S2

	Enzyme activities [nmol/min/mg protein]					
Individual	Citrate synthase	Complex I	Complex II	Complex III	Complex IV	Complex V
F1:II.1	296	46	113	1163	527	468
F4:II.1	245	26	96	946	469	319
F6:II.3	212	33	92	582	544	368
F8:II.1	145	28	76	538	300	264
Control, lower limit	*225*	*18*	*54*	*208*	*270*	*78*
Control, upper limit	*459*	*53*	*124*	*648*	*659*	*287*

Table S2. OXPHOS Enzymes in HPDL Fibroblast Mitochondria Were Normal in Four Affected Individuals (Methods see Table S1)

Table S3

Variant	Location	CDS position	Codons	Protein position	Amino acids	gnomAD AF	SIFT	PolyPhen	CADD PHRED	CADD RAW	PhyloP
ENST00000334815.3: c.149G>A	1:45792969-45792969	149	gGc/gAc	50	G/D	1.018e-05	deleterious (0)	probably_damaging (0.931)	26.8	4.244330	5.78105
ENST00000334815.3: c.469T>C	1:45793289-45793289	469	Tgg/Cgg	157	W/R	4.61e-05	tolerated (0.49)	benign (0.006)	18.01	1.891146	1.06456
ENST00000334815.3: c.503G>A	1:45793323-45793323	503	tGc/tAc	168	C/Y	8.246e-06	deleterious (0)	probably_damaging (0.984)	26.9	4.268768	6.40164
ENST00000334815.3: c.537G>C	1:45793357-45793357	537	tgG/tgC	179	W/C	-	deleterious (0.01)	probably_damaging (0.99)	27.4	4.350300	5.40869
ENST00000334815.3: c.650T>C	1:45793470-45793470	650	cTg/cCg	217	L/P	-	deleterious (0)	probably_damaging (0.983)	26.0	4.080206	4.91222
ENST00000334815.3: c.701T>C	1:45793521-45793521	701	cTt/cCt	234	L/P	5.019e-06	deleterious (0)	probably_damaging (0.99)	25.2	3.849507	5.28457
ENST00000334815.3: c.743T>C	1:45793563-45793563	743	cTg/cCg	248	L/P	-	deleterious (0)	probably_damaging (0.998)	27.9	4.421106	7.14635
ENST00000334815.3: c.753C>A	1:45793573-45793573	753	caC/caA	251	H/Q	-	deleterious (0)	possibly_damaging (0.831)	22.1	2.550874	0.568087
ENST00000334815.3: c.779G>A	1:45793599-45793599	779	gGg/gAg	260	G/E	4.509e-06	deleterious (0.01)	probably_damaging (0.978)	23.4	3.084593	3.67104
ENST00000334815.3: c.797T>C	1:45793617-45793617	797	aTt/aCt	266	I/T	8.506e-06	deleterious (0)	probably_damaging (0.998)	25.2	3.836215	7.14635
ENST00000334815.3: c.859T>C	1:45793679-45793679	859	Tac/Cac	287	Y/H	9.954e-05	deleterious (0)	probably_damaging (1)	26.6	4.214790	7.14635

Table S3. Detailed Information on All Missense Variants Observed in This Study.
The table comprises chromosomal location according to GRCh37/hg19 (Location), coding sequence (CDS position), protein position (Protein position), nucleotide (Codons), predicted amino acid exchange (Amino acids) and gnomAD allele frequency (gnomAD AF). Scores were obtained using the online interface of Ensembl Variant Effect Predictor and 100 vertebrates Basewise Conservation by PhyloP (phyloP100wayAll) in UCSC.[3; 4] Raw values are given in brackets for SIFT and PolyPhen-2, CADD scores are displayed as PHRED-like scores (CADD PHRED) and raw values (CADD RAW). References as provided by Ensembl VEP: SIFT: <0.05 deleterious, ≥0.05 tolerated, PolyPhen: >0.908 probably damaging, >0.446 and ≤0.908 possibly damaging, ≤0.446 benign, CADD PHRED >30 likely deleterious (predicted to be among the 0.1 % most deleterious possible substitutions in human genome). PhyloP: positive scores: conserved nucleotide, negative scores: fast-evolving site.

SUPPLEMENTAL MATERIAL AND METHODS

Cell Culture. Fibroblasts from affected individuals, SV40 large T antigen-immortalized fibroblasts from affected individuals or N2a cells were maintained in DMEM with D-glucose and pyruvate (Gibco), 10 % FBS (Gibco) and 1 % Penicillin/Streptomycin (Gibco). All cells were incubated at 37 °C and kept under 5 % CO_2 atmosphere. Cells were routinely tested for mycoplasm contamination.

***HPDL* cDNA Overexpression in N2A Cells (Figure 2).** *HPDL* cDNA was amplified with Phusion polymerase (Thermo) using primer with overhanging ends containing restriction sites for cloning and the double FLAG-tag in frame. Wild-type HPDL was amplified with HPDL_for GGGagatctGCcgccatggccgcgcccg and HPDL_full_rev gggGCGGCCGCttaCTTGTCGTCATCGTCTTTGTAGTCCTTGTCGTCATCGTCTTTGTAGTCggcttc ctggctcctggcagattgc. PCR products were gel purified and cut with restriction enzymes and placed in the pEGFP-N1 vector. Resulting clones were Sanger sequenced and transfected into near-confluency N2a cells with Lipofectamine P3000 (Thermo). 24 hours following transfection cells were incubated with 100 nM Mitotracker Red CMXRos (Invitrogen) in medium for 45 minutes at 37 °C and fixed with Methanol at -20 °C for 15 minutes. Fixed cells were stained with a rabbit α-FLAG antibody (Sigma Aldrich) and subsequently with a goat α-rabbit-Alexa Fluor 488 antibody (Invitrogen). DAPI staining (Invitrogen) was performed according to the instructions of the manufacturer. Fixed cells were mounted with Fluoromount G (Southern Biotech) and were analysed with a Zeiss LSM 880 confocal microscope.

SUPPLEMENTAL REFERENCES

1. Feichtinger, R.G., Zimmermann, F., Mayr, J.A., Neureiter, D., Hauser-Kronberger, C., Schilling, F.H., Jones, N., Sperl, W., and Kofler, B. (2010). Low aerobic mitochondrial energy metabolism in poorly- or undifferentiated neuroblastoma. BMC Cancer 10, 149.
2. Rustin, P., Chretien, D., Bourgeron, T., Gerard, B., Rotig, A., Saudubray, J.M., and Munnich, A. (1994). Biochemical and molecular investigations in respiratory chain deficiencies. Clin Chim Acta 228, 35-51.
3. McLaren, W., Gil, L., Hunt, S.E., Riat, H.S., Ritchie, G.R., Thormann, A., Flicek, P., and Cunningham, F. (2016). The Ensembl Variant Effect Predictor. Genome Biol 17, 122.
4. Kent, W.J., Sugnet, C.W., Furey, T.S., Roskin, K.M., Pringle, T.H., Zahler, A.M., and Haussler, D. (2002). The human genome browser at UCSC. Genome Res 12, 996-1006.
5. Schindelin, J., Arganda-Carreras, I., Frise, E., Kaynig, V., Longair, M., Pietzsch, T., Preibisch, S., Rueden, C., Saalfeld, S., Schmid, B., et al. (2012). Fiji: an open-source platform for biological-image analysis. Nat Methods 9, 676-682.
6. Valente, A.J., Maddalena, L.A., Robb, E.L., Moradi, F., and Stuart, J.A. (2017). A simple ImageJ macro tool for analyzing mitochondrial network morphology in mammalian cell culture. Acta Histochem 119, 315-326.
7. Zimmermann, F.A., Mayr, J.A., Neureiter, D., Feichtinger, R., Alinger, B., Jones, N.D., Eder, W., Sperl, W., and Kofler, B. (2009). Lack of complex I is associated with oncocytic thyroid tumours. Br J Cancer 100, 1434-1437.